

# Probing Surface Reaction Mechanisms Using Chemical and Vibrational Methods: Alkyl Oxidation and Reactivity of Alcohols on Transition Metal Surfaces

Marcus K. Weldon<sup>†</sup> and Cynthia M. Friend\*

Department of Chemistry, Harvard University, Cambridge, Massachusetts 02138

Received September 1, 1995 (Revised Manuscript Received April 4, 1996)

## Contents

I. Introduction	1391
II. Alcohol Reactions on Transition Metal Surfaces	1392
III. Vibrational Spectroscopy	1393
A. Background and Introduction	1393
B. General Principles	1393
C. Surface Infrared Spectroscopy	1393
D. Electron Energy Loss Spectroscopy	1395
1. Impact Scattering	1396
2. Resonance Scattering	1397
IV. Chemical Fingerprinting and Mechanistic Studies	1397
A. General Considerations in Studies of Surface Reactions	1397
B. Identification of Surface Intermediates: Alkyl Oxidation on Transition Metal Surfaces	1397
V. Studies of Adsorbate Structure and Bonding by Vibrational Spectroscopy	1402
A. Structure of Methoxide Adsorbed on Metal Surfaces	1402
B. Determination of C–O Bond Strength in Adsorbed Methoxide by Surface Overtone Spectroscopy	1407
VI. Summary	1410
VII. Acknowledgments	1410
VIII. References and Notes	1410



Marcus Weldon graduated from King's College, London in 1990 with a Bachelor's degree in Chemistry and Computer Science. He then moved to Harvard University, where he obtained both an M.S. (1992) and Ph.D. (1995), working in the laboratory of Professor Cynthia Friend on the application of surface vibrational spectroscopy to the study of complex heterogeneous processes in catalysis and diamond atomic layer epitaxy. He was awarded the Nottingham Prize by the American Physical Society in 1995 for his thesis work, and is currently a post-doctoral member of technical staff at AT&T Bell Labs, working with Y. J. Chabal on the use of infrared spectroscopy to probe the surface physics and chemistry occurring at the interface of bonded silicon wafers. His interests are manifold; from the application/extrapolation of fundamental science to technologically relevant processes, to the rearing of his genius son, James.

## I. Introduction

A primary aim of chemistry is to develop general, predictive models for classes of reactions. However, in order to realize this goal, a significant body of work must exist on which to base such deductions. This requirement has only recently begun to be fulfilled in the case of *surface* chemistry due, in part, to notable advances in the techniques and analytical tools available to the surface scientist. Consequently, a plethora of detailed studies of the adsorption, desorption, and reaction of small molecules on surfaces have been reported in the literature over the past two decades, so that it is now possible to derive general mechanisms for a range of complex surface reactions. Indeed, such models are of paramount importance because of the relevance to technologies as diverse as heterogeneous catalysis, materials growth and processing, as well as lubrication and wear.



Professor Cynthia Friend is noted for her work in mechanistic surface chemistry. She joined the Harvard faculty in 1982 after serving as a postdoctoral fellow at Stanford University. She earned her B.S. in Chemistry at the University of California, Davis in 1977 and Ph.D. in Physical Chemistry at the University of California, Berkeley (1981). Her work spans the areas of organometallic and physical chemistry.

In this article, we illustrate the methodology for probing complex surface reactions using investigations of alkyl oxidation and alcohol chemistry on

\* Author to whom correspondence should be addressed.

<sup>†</sup> Present address: AT&T Bell Laboratories, 600 Mountain Ave., Murray Hill, NJ 07974.

transition metal surfaces. The main themes will be (1) how to develop a predictive model of reactivity via systematic variation of molecular and surface properties, such as metal-adsorbate bond strengths and (2) the application of surface vibrational spectroscopy to identify intermediates and probe their structures. Selected examples will be used for illustration; it should not be inferred that these case studies necessarily represent the most technologically or fundamentally important, nor that this article contains an exhaustive review of the literature.

We will start with a brief overview of the known surface chemistry of alkoxides, since they are important intermediates along the path to alcohol formation and also can lead to other oxygenates, such as aldehydes, ketones, or organic acids. The product distributions in alkoxide chemistry can largely be understood in terms of metal-oxygen and metal-carbon bond strengths, although important exceptions arise in which the adsorbate structure and *intramolecular* bonds are sufficiently perturbed by the surface so as to dictate the observed reactivity. The primary focus of the discussion will be on the reactions of methanol, as it is undoubtedly the most frequently studied polyatomic molecule on transition metal surfaces. This is due, in part, to the technological importance of the heterogeneous reactivity of such alcohols and the fact that methanol is the smallest member of this class of reagents, so that it has been widely used as a test case for the study of complex surface reactions. However, despite the considerable interest in these systems over the last decade, there is still considerable controversy over the interpretation of the surface vibrational spectra of alkoxides, to the point where some doubt has been cast on the (current) utility of these techniques for all but the simplest adsorbates. Therefore, we will spend some time discussing the relevant excitation mechanisms and selection rules operative in electron energy loss and surface infrared spectroscopy, in which we emphasize aspects that are sometimes overlooked in the literature, contributing to this contention. In addition, we will discuss several experimental configurations or approaches that facilitate the collection of high-quality vibrational data that yield maximal information content. Following this, we will first discuss the use of electron energy loss spectroscopy for adsorbate chemical "fingerprinting" with particular reference to the identification of methoxide formed from reaction of gaseous methyl with oxygen on Rh(111)<sup>1</sup> and Pd(111). Such alkyl oxidation reactions are of great potential importance, because alkyls are thought to play a pivotal role in a variety of processes; most notably, heterogeneous alkane oxidation. We will then go on to detail the use of infrared spectroscopy for the determination of the structure of methoxide adsorbed on Mo(110) using selective isotopic labeling, the results of which are shown to be applicable to CH<sub>3</sub>O- on all metallic surfaces studied to date. Furthermore, an extension of this approach to more complex species such as 2-propoxide is suggested, in which the need for calculations of the interaction potential between the adsorbate and the extended surface, incorporating a full normal mode analysis, is clearly

demonstrated. Finally, we highlight the use of vibrational spectroscopy for the determination of adsorbate bond strength so that surface-induced changes in the intramolecular potentials can be directly probed. In particular, we demonstrate that there is a breakdown in the correlation observed in the condensed phase and organometallic literature between fundamental bond-stretching frequencies and the relevant bond energies.

## II. Alcohol Reactions on Transition Metal Surfaces

The reactions of alcohols, in particular methanol, on transition metal surfaces have been widely studied due to their importance as products of partial oxidation reactions. The O-H bonds of alcohols generally break upon adsorption on metal surfaces at low-surface temperatures, producing an adsorbed alkoxide intermediate, RO-, and surface hydrogen.<sup>2</sup> The subsequent reactions of the alkoxide intermediates exhibit strong periodic trends in the reactivity of the C-O bond, as illustrated using select examples from the literature. Again, an exhaustive review of the literature is beyond the scope of this article.

The C-O bond of alcohols is generally retained on the mid- to late-transition metals, e.g. Cu,<sup>3-5</sup> Ag,<sup>6</sup> Au,<sup>7</sup> Pt,<sup>8-12</sup> Pd,<sup>13-15</sup> Rh,<sup>2,16-20</sup> and Ru.<sup>21,22</sup> The most common reaction of alkoxide intermediates on the latter (group VIII) metal surfaces is direct elimination of CO and H<sub>2</sub>. In contrast, the three noble metals are sufficiently inert that they only cause partial dehydrogenation of the alkoxide (methoxide) intermediate to the aldehyde (formaldehyde) which, in turn, either desorbs or decomposes (on the oxygen-covered surface) via a surface carboxylate species, to CO and H<sub>2</sub>. In fact, no reaction is observed on either Ag or Au in the absence of coadsorbed atomic oxygen, which acts as a Brønsted base, facilitating O-H bond scission. Lastly, longer-chain alkoxides, such as 2-propoxide, undergo C-C bond scission as well as dehydrogenation to yield CO on mid-transition metals, e.g. Pd(111).<sup>13</sup>

The retention of the C-O bonds of alkoxides adsorbed on the mid- to late-transition metals has important mechanistic implications for the selectivity of the ensuing reactions. In particular, the C-H bond adjacent to the oxygen atom, the so-called  $\beta$ -C-H bond, is more readily broken than others in the alkoxides. This is a direct consequence of the withdrawal of electron density from the carbon bound to oxygen such that the  $\beta$ -C-H bond is weaker than others. As a result, selective  $\beta$ -H elimination occurs in a number of cases, e.g. acetone formation from 2-propoxide bound to Rh(111)-p(2 $\times$ 1)-O.<sup>2</sup>

In contrast, the C-O bond in alcohols bound to Mo(110)<sup>23-27</sup> or Fe<sup>28-31</sup> is readily cleaved. For example, the C-O bond in methoxide breaks below 400 K on Mo(110), resulting in  $\sim$ 99% nonselective decomposition to surface carbon, hydrogen, and oxygen.<sup>23</sup> Similarly, the C-O bonds of longer chain alkoxides bound to Mo(110) readily break, leading to olefin elimination. For example, propene is the primary product of the reaction of 2-propoxide on Mo(110), with the oxygen remaining behind on the surface.<sup>25,27</sup> Interestingly, the facility for C-O bond

breaking in alkoxides bound to Mo(110) correlates with the C–O bond strengths in the corresponding gas-phase alcohols.<sup>24–27</sup> Accordingly, the C–O bond of phenoxide breaks at the highest temperature, with primary alkoxides such as ethoxide and 1-propoxide decomposing more readily. Taken together, these data suggest that not only are the C–O bonds in alkoxides strongly perturbed by bonding to the molybdenum, but that homolytic C–O bond breaking is rate determining in the alkoxide reactions on Mo(110).

The periodic trends in the reactivity of alkoxides on transition metal surfaces can be rationalized on the basis of the magnitudes of the metal–oxygen bond strengths estimated for the different surfaces. Taking the average M–O bond strengths as a guide, C–O bond cleavage is expected to be more favorable on molybdenum, which has an extremely strong M–O bond, compared to mid-transition metals, e.g. Rh and Pd, which have intermediate metal–oxygen bond strengths. Similarly, the noble metals exhibit the weakest M–O bonds, consistent with the complete retention of the O–H bond (and absence of reaction) on the clean Cu, Ag, and Au surfaces. While this correlation generally holds, there are a few exceptions. Specifically, C–O bond breaking in methoxide bound to the reconstructed Pt(110)-(2×1) surface was reported,<sup>32</sup> and the C–O bond in methoxide bound to Mo(100) is retained.<sup>33</sup> These exceptions demonstrate that surface geometric and/or site-specific electronic effects may also play an important role in determining the reactivity. Alternatively, the relative binding energies of the other surface species produced by reaction, such as CO<sub>(a)</sub>, H<sub>(a)</sub>, or CH<sub>3(a)</sub> may also play a role.<sup>8</sup>

Clearly, in order to more fully understand the periodic trends in alkoxide reactivity, systematic studies of the bonding and structure of alkoxides are necessary. In sections IV and V, detailed spectroscopic investigations of alkoxides on Mo(110) are described. Similar investigations on selected late- and mid-transition metal surfaces where the chemistry is well characterized have also appeared in the literature over the last few years, so that a more complete understanding of the periodic trends in alkoxide chemistry is beginning to emerge. In this article, the sole focus will be the role of vibrational spectroscopy as a chemical and structural probe, although a variety of other techniques such as near-edge X-ray absorption fine structure spectroscopy (NEXAFS) and electron-stimulated desorption ion angular distribution (ESDIAD) have been successfully employed in the literature for some systems. Of particular note is the recent refinement of photoelectron diffraction techniques by Bradshaw and Woodruff,<sup>34–36</sup> for the study of adsorbate species. This technique promises not only to provide adsorbate structural information but also to reveal the specific binding site on the surface, so that the potential importance of this approach cannot be overstated. However, there is one major drawback, in that a synchrotron source is required to produce the variable-energy soft X-rays necessary for the (preferred) scanned-energy mode of operation. Consequently, this technique cannot be widely implemented in

surface science laboratories, so that vibrational spectroscopies will continue to be essential structural probes for the foreseeable future. In fact, the interpretation of surface vibrational spectra is greatly facilitated by recourse to such structural information, so that the relationship between the two techniques may ultimately be symbiotic in nature.

### III. Vibrational Spectroscopy

#### A. Background and Introduction

Vibrational spectroscopies, namely high-resolution electron energy loss and infrared reflection absorption spectroscopy, have been increasingly used to study surface phenomena, primarily as a result of significant advances in instrumentation and in the theoretical description of surface phenomena over the past 20 years. Consequently, a detailed microscopic picture of the relevant physics and chemistry occurring at interfaces has begun to emerge; the wealth of information that has been derived to date is detailed in a series of excellent reviews on the subject that are highly recommended to the reader.<sup>37–41</sup> In contrast, this article is not intended to serve as a comprehensive review of the existing literature; instead, we have selected a few specific examples that highlight developing areas of surface vibrational spectroscopy from a *chemical* perspective. The examples chosen illustrate the methodology for tackling chemically complex problems, while underscoring the need for complementary studies using other structural probes as well as detailed theoretical treatments, in order to gain a more complete understanding of complex heterogeneous systems.

#### B. General Principles

Careful interpretation of vibrational data is crucial to understanding chemical bonding to surfaces since significant energy shifts and changes in coupling will inevitably occur upon chemisorption. This is particularly true for spectra obtained with the use of electron energy loss spectroscopy where multiple loss mechanisms can be operative, each with specific selection rules,<sup>37</sup> which are all too often overlooked or ignored. Indeed, even with infrared spectroscopy, for which only dipole excitation is possible, the experimental configurations or protocols typically adopted do not allow full utilization of the resolution and sensitivity available. Therefore, we review a few of the basic aspects of each technique. We stress, however, that this should not in any way be considered a definitive text in this regard—there are several superb comprehensive reviews.<sup>38–41</sup> Herein, we emphasize those aspects of electron energy loss and infrared absorption spectroscopies that are of particular importance in interpreting spectra of chemically complex surface species.

#### C. Surface Infrared Spectroscopy

Fresnel's equations can be used to demonstrate that only at grazing angles of incidence (typically  $\phi = 85–88^\circ$  with respect to the surface normal) of the infrared beam is there any significant component of the electric field at a metal surface, due to the large

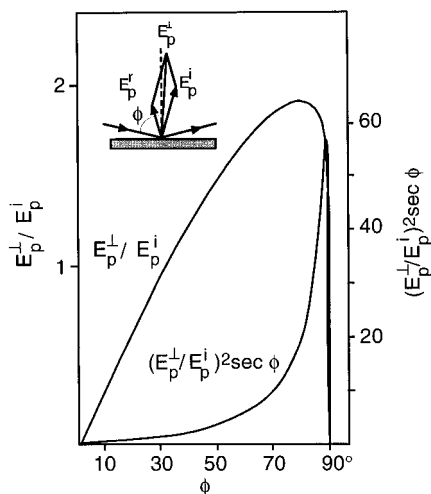


**Figure 1.** The relative amplitude of the electric field normal to a metal surface, as a function of angle of incidence  $\phi$  (with respect to the surface normal), together with the square of this quantity scaled by  $\sec \phi$ , which gives the relative sensitivity for a (perpendicular) dipole. (Taken from Hayden, ref 38.)

dielectric constants and consequent excellent screening properties of nearly all metals. Indeed, the only nonvanishing component of the electric field is perpendicular to the metal surface and approaches a value of  $2E_0$  (where  $E_0$  is the incident electric field intensity) at the optimum angle of incidence, before decaying to zero at larger angles due to the destructive interference between the incident and reflected beams that are  $180^\circ$  out of phase for a beam exactly parallel to the surface plane (Figure 1). Consequently only modes that give rise to a dynamic dipole moment normal to the metal surface can be vibrationally excited—the so-called “Surface Dipole Selection Rule”. Furthermore, by consideration of the symmetry properties of the vibrational wave functions involved, the following refinement arises: only transitions to excited states that transform as the totally symmetric representation of the symmetry group are allowed. This is a consequence of the form of the transition matrix element, which is the product of the initial and final states and the dipole moment operator. The surface dipole selection rule requires that  $\mu = \mu_z$ , where  $\mu_z$  is necessarily totally symmetric with respect to all the symmetry operations of any surface symmetry group. Therefore, since the ground state (the only initial state with a significant population at temperatures  $\leq 300$  K) of a harmonic oscillator is always totally symmetric, the excited state must also be totally symmetric, in order for the transition dipole moment to be nonvanishing. However, there is an important corollary to this last statement; that is the requirement that the excited state is totally symmetric is a necessary but *not sufficient* condition for observation of a mode. Consider the symmetric stretching vibration of the hypothetical molecule depicted in Figure 2; this motion is totally symmetric with respect to the operations of (at least) the  $C_{2v}$ ,  $C_s$ , and  $C_1$  surface symmetry groups, yet has no component of the dipole moment perpendicular to the surface and, therefore, would not generally be experimentally observable using surface infrared spectroscopy. In some cases, this motion may be accompanied by a change in the

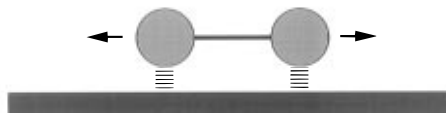


**Figure 2.** Schematic depiction of a symmetric stretching mode of a diatomic adsorbate parallel to the surface plane.

charge density between the metal and the adsorbate, creating a dynamic dipole moment normal to the surface, such that the mode is then “surface dipole allowed”. This phenomenon is most prevalent for species such as ethylene which often adsorb with the C=C bond axis parallel to the metal surface and bond via a combination of donation of  $\pi$ -electron density to the metal and “back-donation” from filled metal states into the  $\pi^*$  molecular orbitals of the adsorbate. The bonding interaction is expected to be a sensitive function of the C=C bond length, so that a dipole moment normal to the surface may develop as the C=C bond vibrates, due to the modulation of electron density in and out of the surface.

Now, since all first harmonics transform as the normal coordinate over which they execute motion, simple inspection of the atomic motions associated with a given mode type (i.e. symmetric or asymmetric stretching, bending, rocking, etc.) will usually suffice to elucidate the surface dipole activity for a given symmetry group. In addition, all second harmonics (first overtones) of nondegenerate fundamentals are always totally symmetric and therefore surface-dipole allowed; this is not always true in the case of overtones of *degenerate* fundamentals, so that the character of the overtone mode must be evaluated for each mode and symmetry group. Importantly, the actual observation of first overtones requires either electrical or mechanical anharmonicity in the system, just as in the condensed phase, where the former refers to the existence of second (and higher)-order terms in the expansion of the adsorbate dipole moment,  $\mu_z$ , and the latter to the presence of third (and higher)-order terms in the Taylor series expansion of the adsorbate potential energy surface. Mechanical anharmonicity has the effect of coupling together the harmonic oscillator normal modes, since these modes do not diagonalize the higher order terms in the potential, so that the modes are more correctly described as a mixture of the harmonic normal modes. Indeed, it is this “mixing” of modes that leads to the phenomenon known as Fermi resonance, where the overtone of one mode mixes with the *near-degenerate* fundamental of another, thereby gaining intensity as detailed in section IV.A.

As a result of the above discussion it might, on first inspection, appear to be a nontrivial task to determine precisely which harmonic normal modes are allowed and which are not. However, there are once again strict symmetry requirements on this mode mixing, as follows: the coupling is described by a matrix element of the form  $\langle \Psi_a | V_{\text{anh}} | \Psi_b \rangle$ , where  $\Psi_a$  and  $\Psi_b$  are the wave functions of two harmonic normal modes and  $V_{\text{anh}}$  includes all the third and higher order terms in the potential energy. Importantly, these anharmonic terms must be totally symmetric with respect to the operations of the relevant symmetry group, so that in order for this

matrix element to be nonzero, only states of the same symmetry can be coupled. Furthermore, the *strength* of the coupling will depend on both the anharmonicity and the relative energies of the states involved, so that coupling is usually only significant between near-degenerate modes, as in the case of the overtones of the deformation and C–H stretching modes of methyl-containing species (section V.A). In such cases, the intensity of the nominal overtone state is often derived *exclusively* from the component of the allowed fundamental with which it is mixed, so that these modes can possess considerable intensity, and may even dominate a given spectral region.<sup>42</sup> In contrast, although electrical anharmonicity can also give rise to the excitation of totally symmetric overtone modes, even in the absence of mechanical anharmonicity, the intensity is proportional to the square of the second derivative of the dipole moment with respect to the normal coordinate involved, which is usually small; typically  $\sim 1\%$  of the intensity of the fundamental (section V.B).

We now proceed to consider some experimental aspects relevant to surface infrared spectroscopy. The use of Fourier transform infrared (FTIR) spectrometers has proliferated over the past few years, at the expense of conventional dispersive (grating) instruments. This is due, primarily, to the increase in throughput when one does not have to use narrow slits (the Jacquinot advantage) and the “multiplex” or Fellgett advantage which results from the acquisition of an entire spectrum in a single scan. Importantly, dispersive instruments may still possess considerable advantages in the mid-IR region, where the signal-to-noise is limited by the so-called “fluctuation noise” since this scales with the spectral power detected (see, for example, the excellent review by Hayden<sup>38</sup> and references therein). However, the focus here will be on FTIR, although much of the discussion is also relevant to dispersive instruments.

The majority of FTIR spectrometers that are commercially available are all capable of resolutions approaching  $1\text{ cm}^{-1}$ , corresponding to a moving mirror path length of 1 cm. Despite this, much of the data reported in the literature is recorded with a resolution of  $4\text{ cm}^{-1}$ , probably due to the advantages in signal-to-noise ratio for a given scan time, offered by the lower resolution. It is also possible that this is due to the belief that typical vibrational half-widths are on the order of  $10\text{ cm}^{-1}$ , so there is little to be gained by operating at higher resolution. However, in a significant percentage of the adsorbate systems we have studied (none of which formed ordered overlayers), additional features were resolved by scanning at either 2 or  $1\text{ cm}^{-1}$  resolution, particularly in the case of methoxide adsorbed on Mo(110) (section V.A). Therefore, it would be surprising if the same were not true for other adsorbate–substrate combinations, given the similarity between the data obtained at  $4\text{ cm}^{-1}$  for  $\text{CH}_3\text{O}^-$  on Mo(110) and that reported for other surfaces (see Figure 12). An obvious concern that arises with the increase in scan time required to obtain the same signal-to-noise at  $2\text{ cm}^{-1}$  resolution as is observed at  $4\text{ cm}^{-1}$ , is the increase in fluctuation noise which results from the

variation in quantities such as detector sensitivity, source intensity and sample position, with time. Indeed, Hayden<sup>38</sup> has suggested that these factors are largely responsible for the noise component obtained in the  $1000\text{--}4000\text{ cm}^{-1}$  region, so that elimination or minimization of these effects is obviously of prime concern to the surface infrared spectroscopist. Fortunately, a good data collection protocol can significantly offset the effect of these temporal fluctuations; for example if the number of scans of an overlayer/background is *reduced*, and then a number of *identical* experiments performed and co-added together, the longer term drift components to the fluctuation noise can be minimized. Furthermore, by selectively co-adding the series of spectra, noise arising from short-term temporal instability or spurious signals, which may occur due to interference effects from external sources or atmospheric conditions, can also be reduced. However, a word of caution is necessary: the major disadvantage of this approach (other than the increase in sample preparation time) is that great care has to be taken to ensure that spectra of *exactly* the same overlayer are averaged; one way to ensure this is to reference each “acceptable” sample scan to another—the result should obviously approximate a straight line at zero absorbance.

Finally, one experimental component that is desirable (but often omitted) is a polarizer. The reason for this is essentially intuitive, as follows: in the absence of a polarizer, photons that are predominantly s-polarized are being emitted by the source and subsequently collected by the detector with zero absorbance, due to the vanishing electric field at the surface, yet they are being averaged in with the p-polarized photons which contain the real experimental signal. This not only results in a smaller measured absorbance ( $= \log I/I_0$ ) and lower signal-to-noise, but will obviously give erroneous values for the deduced vibrational polarizability of the adsorbate, a quantity of central importance in any theoretical analysis of the interadsorbate coupling.

## D. Electron Energy Loss Spectroscopy

The above discussion of dipole excitation of surface vibrational modes is also applicable to electron energy loss spectroscopy as it is often the predominant loss process for on or near-specular detection angles using this technique. A detailed review of the physical basis of high-resolution electron energy loss spectroscopy is presented in Ibach and Mills' definitive text.<sup>37</sup> The actual loss maximum of a dipole-scattered feature is typically a few degrees off-specular in the scattering plane, due to the small (but nonzero) momentum transfer that is involved.<sup>37,38</sup> Indeed, this fact can be used to definitively distinguish between dipole scattering and other possible loss mechanisms in electron energy loss spectroscopy. In fact, there are two additional loss mechanisms operative when low-energy electrons, as opposed to photons, are used to probe the vibrational structure of adsorbate systems; namely “impact” and

“resonance” scattering, that may contribute significant intensity in off-specular directions, both in and out of the scattering plane. In addition, under certain circumstances that are discussed below, these processes may also give rise to significant intensity *on*-specular. Importantly, both of these processes have specific selection rules that apply, as well as characteristic angular and energy distributions that are worthy of some consideration in order that spectra are correctly interpreted. All of the elements of the following discussion can be found elsewhere in the literature, we have simply summarized what we feel are the most pertinent issues for studies of complex adsorbates.

### 1. Impact Scattering

Impact scattering is usually described as a short-range interaction, as it is due to the inelastic scattering of the incident electrons from the ion cores, by a process that involves the same interaction potential as for the diffracted electrons observed in low-energy electron diffraction (LEED). A consequence of the large momentum transfer inherent to such inelastic processes is a broad angular distribution of the scattered electrons, which lowers the number of electrons scattered into any given solid angle, but can be used to identify an impact loss feature. In addition, inspection of the functional form for the scattered intensity suggests that overtone excitation should be enhanced by impact scattering, although the presence of multiple-loss features (at  $n\omega_0$ , where  $n = 1, 2, 3 \dots$ ) that result from the loss of a quantum of energy at each of  $n$  different scattering centers may effectively hinder the resolution of the genuine overtone in the absence of appreciable mechanical anharmonicity. The cross section for impact scattering increases with incident electron energy, in contrast to the decrease with increasing  $E_i$  observed for dipole scattering (inherent to such Coulombic processes), so that at high incident electron energies, impact scattering will be the dominant loss process. However, the electron energies required for this to be the case are typically on the order of 50 eV, which is beyond the range of most spectrometers. Therefore, over the 1–10 eV range that is routinely accessible, the dipolar cross section is typically a factor of 100 greater than that for impact scattering for a strong dipole scatterer (e.g. C–O or C–F containing species), when the relative angular distributions are taken into account. It is important to recognize that this value may be significantly reduced (and even approach unity) for higher frequency modes (e.g. C–H, N–H, or O–H stretching modes) or for weak dipole scatterers since the ratio of impact to dipolar intensity is proportional to the vibrational frequency, and inversely proportional to the relative effective charge associated with a mode.<sup>37</sup>

So far, we have said nothing about the selection rules operative for impact scattering which, by their very nature, modify the conditions under which impact losses are observed. By time reversal arguments,<sup>37,43</sup> it can be shown that any mode that is antisymmetric with respect to a plane of symmetry

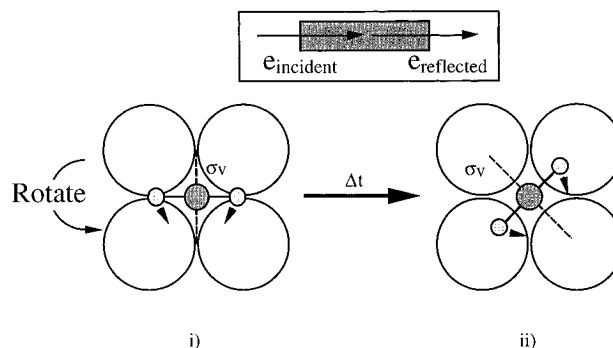


**Figure 3.** Plan view of the bending mode of a linear triatomic (XYX) species adsorbed parallel to the surface plane and undergoing rotation about the 2-fold symmetry axis. In i the bending mode is antisymmetric with respect to the mirror plane that lies in the scattering plane, so that it is totally impact forbidden for detection in this plane. However, as the molecule rotates to ii, the mirror planes are no longer parallel to the scattering plane and therefore the mode becomes impact allowed (off-specular) in this plane.

of the adsorbate–substrate complex that is also either (i) in the scattering plane, or (ii) in the plane perpendicular to it, will be impact forbidden in the specular direction. In the latter case the mode is allowed *off*-specular in the scattering plane, in contrast to situation i, when the mode is only allowed *off*-specular *out of the scattering plane*. Third, if a vibrational mode is antisymmetric with respect to a 2-fold axis of the relevant symmetry group, it is forbidden in the specular direction, but allowed *off*-specular. Note that a variety of different possibilities exist where these selection rules do not significantly limit the observation of impact-scattered modes, either on- or off-specular:

(i) For the lowest adsorbate symmetry possible ( $C_1$ ) there are no 2-fold elements or mirror planes, so that all modes are impact-allowed, for all scattering directions *including the specular direction*. Therefore, the assumption that impact scattering only contributes intensity away from the specular direction is clearly not valid for such low-symmetry adsorbate overlayers.

(ii) Even for the most ordered overlayers, if the scattering plane is not aligned either parallel or perpendicular to any symmetry plane of the adsorbate–substrate complex, then only the third selection rule will be operative, such that all modes will be impact-allowed *off*-specular in the scattering plane.

(iii) Alternatively, if the overlayer is disordered so that multiple adsorbate configurations exist, then only a fraction of these species will have symmetry planes that are aligned as required by the selection rules i and ii above, so that once again the third rule will dominate, resulting in all modes being impact-allowed away from the specular direction.

(iv) A final, intriguing possibility is that if there is rotation about the symmetry axis of a molecular adsorbate on the time scale over which the relevant spectral region is scanned, the adsorbate symmetry planes change their relative disposition to the scattering plane as a function of time, as illustrated in Figure 3. Consequently, these modes will be (partially) impact-scattered despite being forbidden in the static limit.

In summary, from the above discussion it is clear that a judicious choice, or at least knowledge of the orientation of the scattering plane with respect to the low index planes of a single-crystal metal surface, coupled with on- and off-specular data collection, significantly enhance the information content provided by the impact-scattering mechanism.

## 2. Resonance Scattering

The final scattering mechanism that can give rise to vibrational excitation in electron energy loss spectroscopy is "resonance" scattering or temporary negative ion formation, which may occur when an incident electron is transiently trapped in an adsorbate "shape-resonance" or virtual excited state. This trapping instantaneously changes the electron density between the nuclei, which, if they are not at their equilibrium configurations with respect to the new electronic charge distribution, respond by moving under the influence of this restoring force until the excited state electron is reejected into the vacuum and the adsorbate returns to the ground-state potential energy surface. Once again, there are characteristic energy and angular distributions as well as selection rules that apply to the resonance-scattering process, the most important of which is perhaps the sensitivity to electron energy that is inherent to any resonant process. The impact energy dependence alone should be sufficient to identify a resonance-scattered loss feature since, as detailed above, the efficiency of dipole scattering generally decreases monotonically, and that for impact scattering increases monotonically with increasing electron energy. In contrast, the resonance scattering intensity is usually a relatively sharply peaked function of electron energy, with a half-width on the order of a few electronvolts. In addition, the angular distribution reflects the symmetry of the excited electronic state and is invariant with electron energy (other than the attendant attenuation away from the resonant energy). Importantly, the cross section of such resonance excitations is typically 2 orders of magnitude greater than for impact scattering, so that they can be comparable in intensity to dipolar losses. Furthermore, the intensity of overtone modes is also enhanced in the resonance scattering regime, due to the large-amplitude displacements that are typical during such electronic transitions. Finally, we consider the applicable selection rules; since the restoring force is proportional to the square of the wave function of the trapped electron, only those modes that transform as the direct product of the excited-state wave function with itself can be excited by resonance scattering.<sup>37</sup> Now, although this would appear to require knowledge of the symmetry of the excited state, there is an essential simplification that arises: if the adsorbate symmetry group does not contain degenerate representations (i.e.  $C_{2v}$ ,  $C_s$ , or  $C_1$ ) the direct product of any irreducible representation with itself is necessarily totally symmetric so that, once again, only totally symmetric modes can be resonance-excited, independent of the scattering geometry.

## IV. Chemical Fingerprinting and Mechanistic Studies

### A. General Considerations in Studies of Surface Reactions

The examples presented below illustrate how a general class of reactions can be probed using chemical techniques. Specifically, we show that a broad understanding of surface reaction mechanisms can be attained by systematic variation of molecular functional groups and comparison of data obtained for metals with different geometric and electronic structures. Furthermore, a key part of the characterization of such heterogeneous systems is the selection of the appropriate combination of spectroscopies and methodologies aimed at identifying intermediates and probing adsorbate structure.

Vibrational spectroscopies have played a key role in identifying a wide variety of intermediates in surface reactions. The use of vibrational "fingerprints" in identifying surface species is similar to the approach widely used by chemists for homogeneous systems. The primary difference in the case of surface intermediates is that reference spectra must generally be obtained on the surface of interest because of the possibility of large surface-specific energy shifts that may otherwise prevent definitive mode assignments. In addition, isotopic labeling experiments are generally critical for unambiguous vibrational assignments. Our investigations of methyl radicals with oxygen-covered Rh(111) will be used to illustrate our experimental approach to the identification of surface intermediates using vibrational spectroscopy.

High-resolution electron energy loss spectroscopy is generally the technique of choice for identifying surface intermediates because of its large spectral range and generally higher sensitivity, compared to infrared reflection absorption spectroscopy. For chemical fingerprinting, the multiple scattering mechanisms operative in electron energy loss spectroscopy are also generally advantageous, since they serve to enhance the intensities and number of loss features observed. In addition, the lower resolution of an electron energy loss experiment is usually not a severe impediment to the identification of surface intermediates, although subsequently, more detailed analyses of adsorbate structure and bonding may be necessary, using an alternative technique such as surface infrared spectroscopy.

In this section, we will detail the use of electron energy spectroscopy for "chemical fingerprinting" of partial oxidation reactions on metal surfaces and the consequent mechanistic deductions that can be made by a combination of vibrational techniques and temperature-programmed reaction data, before proceeding to consider the "higher-order" aspects of surface vibrational spectra in section V.

### B. Identification of Surface Intermediates: Alkyl Oxidation on Transition Metal Surfaces

Alkyl oxidation is most certainly an important step in alkane oxidation, one of the preeminent problems

in heterogeneous catalysis today. There is general agreement that the first, and rate-determining, step in alkane oxidation is the homolytic cleavage of a C–H bond to generate the corresponding alkyl radical. Therefore, an understanding of the chemistry of alkyl radicals is crucial to developing models of alkane reactivity.

Clearly, the investigation of alkyl oxidation requires studies of both surface-bound alkyls and the interaction of gaseous alkyl radicals with surfaces. Notably, alkyls bound to surfaces are no longer true radical species since a strong metal–R bond is formed, despite the misuse of the term “radical” in the literature.<sup>44a,b</sup> Most commonly, heterogeneous dissociation of the relatively weak C–I bonds in alkyl halides has been used to generate surface-bound alkyls, as described in detail in the companion article by B. E. Bent.<sup>45a–f</sup> However, surface-bound methyl has also been synthesized using methane dissociation induced by high impact energies and identified using electron energy loss spectroscopy.<sup>44a,b,46–51</sup> In addition, *gas-phase* methyl radicals have been generated by pyrolysis of azomethane, allowing for study of reactions between R<sup>•</sup> and surface oxygen.<sup>1,52,53</sup>

Importantly, the heterogeneous dissociation of alkyl halides on metal surfaces is inhibited by surface oxygen in the two cases reported in the literature: Rh(111)<sup>54–56</sup> and Pd(100).<sup>57</sup> Therefore, photodissociation has been used to circumvent the problem of thermal C–I bond dissociation in recent investigations of alkyl halides on metal surfaces (as reviewed by White et al.),<sup>58</sup> and on oxygen-covered Pd(100)<sup>57</sup> and Rh(111).<sup>59</sup> Alternatively, thermal C–I bond dissociation could (in principle) be carried out on the clean surface, followed by oxygen adsorption so as to investigate this class of reactions. However, recent investigations of gas-phase methyl radicals with Rh(111) demonstrate that direct addition to adsorbed oxygen is facile, while adsorbed methyl does *not* react with surface oxygen, as described below (Figure 4).<sup>1</sup>

High-resolution electron energy loss spectroscopy was used to demonstrate that gas-phase methyl radicals react directly with surface oxygen to form adsorbed methoxide on Rh(111).<sup>1</sup> Specifically, the surface methoxide species was identified on the basis of the intense C–O stretch at 975 cm<sup>-1</sup>, clearly evident following reaction of <sup>•</sup>CH<sub>3</sub> with adsorbed oxygen (Figure 4d). The isotopic shift measured when the reaction was carried out on <sup>18</sup>O-labeled Rh(111) provided supporting evidence that the 975 cm<sup>-1</sup> peak was indeed the  $\nu(\text{C–O})$  of adsorbed methoxide, since the observed frequency shift of –35 cm<sup>-1</sup> is in good agreement with that expected upon <sup>18</sup>O-substitution in CH<sub>3</sub><sup>16</sup>O–, assuming a harmonic potential.

The predominance of a surface methoxide intermediate following exposure of oxygen-covered Rh(111) to methyl radicals was further confirmed by reference to data obtained for methoxide formed from methanol decomposition on clean and oxygen-covered Rh(111) (Figure 4).<sup>1,18,19</sup> High-resolution electron energy loss spectra have been used to show that the O–H bond in alcohols breaks upon adsorption at <120 K on a wide variety of metal surfaces, including Rh(111).<sup>60</sup> Specifically, the absence of the O–H stretch following

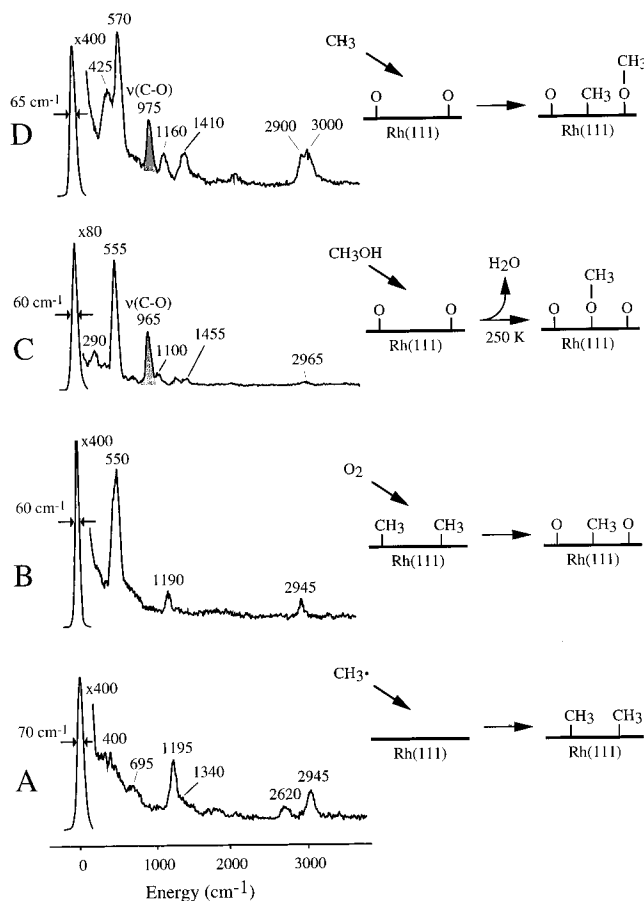


**Figure 4.** High-resolution electron energy loss spectra: (a) methyl adsorbed on clean Rh(111); (b) after exposure of CH<sub>3</sub>/Rh(111) to molecular oxygen; (c) methoxide formed from methanol dissociation at 120 K on oxygen-covered Rh(111); and (d) a mixture of methoxide and methyl formed from reaction of gaseous methyl radicals with surface oxygen on Rh(111)-p(2 × 1)-O. (From ref 1.)

alcohol adsorption is taken as evidence of O–H bond scission. Generally, the  $\nu(\text{O–H})$  loss in adsorbed alcohols is expected to have a large contribution from impact scattering,<sup>37</sup> so that the O–H stretch mode should be observed *even* for parallel orientations that may render the mode dipole forbidden. In this way, electron energy loss spectroscopy provides clear evidence that the O–H bond in methanol is broken at low temperature on Rh(111), for example (Figure 4c), given that the O–H stretching mode in condensed methanol is at ~3260 cm<sup>-1</sup>,<sup>23</sup> and no mode is observed in this region following methanol adsorption on Rh(111) at 120 K. Furthermore, the remainder of the vibrational spectrum clearly indicates that the rest of the molecular framework is uncompromised, since all modes can be assigned to an intact CH<sub>3</sub>O– species bound to the rhodium surface. Specifically, the peaks at 965, 1455, and 2965 cm<sup>-1</sup> are assigned to  $\nu(\text{C–O})$ ,  $\delta_s(\text{CH}_3)$ , and  $\nu(\text{CH}_3)$ , respectively, whereas the peak at ~555 cm<sup>-1</sup> is assigned to the Rh–O stretch of oxygen bound to Rh(111) based on comparison to vibrational data for ordered oxygen layers on Rh(111). Additional coverage-dependent studies of methanol on Rh(111), demonstrate that there are slight shifts in the C–O stretch frequency as the methoxide coverage is changed: the  $\nu(\text{C–O})$  frequency of adsorbed methoxide ranges between 960–980 cm<sup>-1</sup>, depending on the specific coverages of



methoxide and oxygen. Taken together, these reference data unequivocally identify methoxide as a product of gaseous methyl radicals reacting with oxygen on Rh(111).

Vibrational spectroscopy also indicates that not all of the methyl radicals react with oxygen to form methoxide; some adsorb to Rh atoms, forming an equilibrated methyl group on the surface. The relative amounts of methyl and methoxide formed depend on the initial amount of oxygen on the surface, with the amount of methoxide formed increasing approximately linearly with oxygen coverage. Adsorbed methyl is identified on the basis of the characteristic  $\delta_s(\text{CH}_3)$  mode at  $1160\text{ cm}^{-1}$ , which is in good agreement with the observation of an analogous loss at  $1195\text{ cm}^{-1}$  following exposure of the clean Rh(111) surface to gaseous  $\cdot\text{CH}_3$  (Figure 4a,d).<sup>1,61</sup> Importantly, adsorbed methyl is known to exhibit a characteristically low  $\delta_s(\text{CH}_3)$  frequency ( $1150\text{--}1250\text{ cm}^{-1}$ ) that is a sensitive function of coverage and the chemical state of the surface<sup>62</sup> (e.g. the presence of coadsorbed I, O, S), consistent with the observed  $35\text{ cm}^{-1}$  difference between the frequencies on clean and oxygen-covered Rh(111). Indeed, a similar methyl deformation frequency was also reported following  $\text{CH}_3\text{I}$  dissociation on Rh(111), providing additional confirmation of the above assignments.<sup>63</sup>

A similar methodology has been used to show that oxygen does not insert into the Rh-CH<sub>3</sub> bond when methyl is first bound to Rh(111) and oxygen is subsequently adsorbed. Specifically, there is no peak detected in the range of  $960\text{--}980\text{ cm}^{-1}$  that would be associated with the C-O stretch of methoxide (Figure 4b). Indeed, only peaks due to adsorbed methyl and atomic oxygen are present: the  $\nu(\text{Rh-O})$  mode at  $550\text{ cm}^{-1}$ , the  $\delta(\text{CH}_3)$  at  $1190\text{ cm}^{-1}$  and the  $\nu(\text{CH}_3)$  at  $2945\text{ cm}^{-1}$ . These data further confirm that oxygen is dissociatively adsorbed on the Rh(111) surface, even when methyl is initially present on the surface since there are no peaks that can be assigned to the  $\nu(\text{O-O})$  stretch, which is known to occur at  $650\text{ cm}^{-1}$  on Rh(111).<sup>64</sup>

Electron energy loss spectroscopy is clearly an excellent means of identifying surface species produced during a chemical reaction, due to the large number of losses typically excited by the various scattering mechanisms and the high sensitivity to the low-frequency substrate-adsorbate modes. In contrast, the frequency region below  $900\text{ cm}^{-1}$  is very difficult to access with laboratory infrared spectrometers, due to significant attenuation of the glowbar source intensity below this frequency. Indeed, although synchrotron-based facilities have recently been developed to enhance the sensitivity in this low-frequency regime, these methods are not widely available to the surface chemist and are, therefore, not practical for routine species identification. Furthermore, even in the  $1000\text{--}4000\text{ cm}^{-1}$  region of the infrared spectrum, where the majority of the intramolecular modes of interest to the surface chemist occur and the signal-to-noise ratio of conventional spectrometers is optimal, the vibrational modes of some (simple) adsorbate species such as  $\text{C}_x\text{H}_y(\text{a})$ , may be beyond the detection limit of infrared spectroscopy. Fortunately, a wide variety of adsorbates do exist for

which a significant number of vibrational modes are observable using conventional (commercially available) infrared spectrometers, so that the high resolution available using surface infrared spectroscopy can be utilized to probe the precise structure and bonding of surface intermediates, as described in section V.

The final part of this section will review the considerable mechanistic information that can be derived by consideration of the above vibrational data in combination with temperature programmed reaction spectroscopy, even in the absence of detailed analyses of the adsorbate structure and intramolecular bond strengths.

As discussed above, methoxide is formed at low temperature ( $120\text{ K}$ ), via addition of the methyl radical to oxygen adsorbed on the Rh(111) surface. In contrast, methoxide is *not* formed when methyl is first adsorbed onto Rh(111) followed by adsorption of oxygen, for any combination of oxygen and methyl coverages investigated, even though the oxygen was dissociatively adsorbed in all cases, as indicated by the characteristic  $\nu(\text{Rh-O})$  stretch at  $\sim 560\text{ cm}^{-1}$  in the electron energy loss spectrum. However, a similar set of gaseous products were formed during temperature programmed reaction of both  $[\cdot\text{CH}_3 + \text{O}(\text{a})]$  and  $[\text{O}_2 + \text{CH}_3(\text{a})]$  on Rh(111). Specifically, carbon dioxide, CO, H<sub>2</sub>O, and H<sub>2</sub> were all produced, albeit with different reaction kinetics. Therefore, the reactivities of (i) methoxide and (ii) atomic carbon and oxygen on Rh(111) were also independently investigated so as to identify the characteristic evolution temperatures of the different reaction pathways. For example, methoxide was formed by reaction of methanol on clean and oxygen-covered Rh(111) and found to dehydrogenate to produce gaseous CO and CO<sub>2</sub> upon heating, with similar peak temperatures ( $440$  and  $400\text{ K}$ , respectively) to those observed for the reaction of  $\text{CH}_3\cdot$  on oxygen-covered Rh(111), again consistent with methoxide being the predominant surface intermediate in this case (Figure 5a).<sup>19,64</sup> Similar studies performed on mixed layers of  $\text{C}_{(\text{a})}$  and  $\text{O}_{(\text{a})}$  on Rh(111) (generated by first forming atomic carbon from hydrocarbon decomposition and subsequently adsorbing oxygen)<sup>55</sup> resulted in CO and CO<sub>2</sub> evolution above  $500\text{ K}$ ; essentially identical kinetics to those observed during reaction of  $[\text{O}_2 + \text{CH}_3(\text{a})]$ , thereby confirming that adsorbed methyl first dehydrogenates to  $\text{C}_{(\text{a})}$  and subsequently reacts with oxygen on Rh(111) (Figure 5 b). Finally, a trace amount of formaldehyde formation was also observed following reaction of gaseous methyl with Rh(111)- $\text{p}(2\times 1)\text{-O}$  ( $\theta_{\text{O}} = 0.5$ ); a product that was notably absent following reaction of oxygen with surface-bound methyl on Rh(111).<sup>65</sup>

The above observations are also consistent with the observed reactivity of alkyl iodides on oxygen-covered Rh(111)<sup>54</sup> and Pd(100) as follows:<sup>57</sup> At low oxygen coverages ( $\theta_{\text{O}} < 0.25$ ), the I-CH<sub>3</sub> bond breaks at low temperatures ( $\sim 100\text{ K}$ ), primarily giving rise to adsorbed methyl and atomic iodine. Adsorbed CH<sub>3</sub> subsequently dehydrogenates yielding  $\text{C}_{(\text{a})}$ , some of which will react with available  $\text{O}_{(\text{a})}$ . As the oxygen coverage is increased ( $\theta_{\text{O}} > 0.25$ ), C-I bond dissociation is sufficiently inhibited by the coadsorbed oxygen that it becomes rate-limiting. This results in an

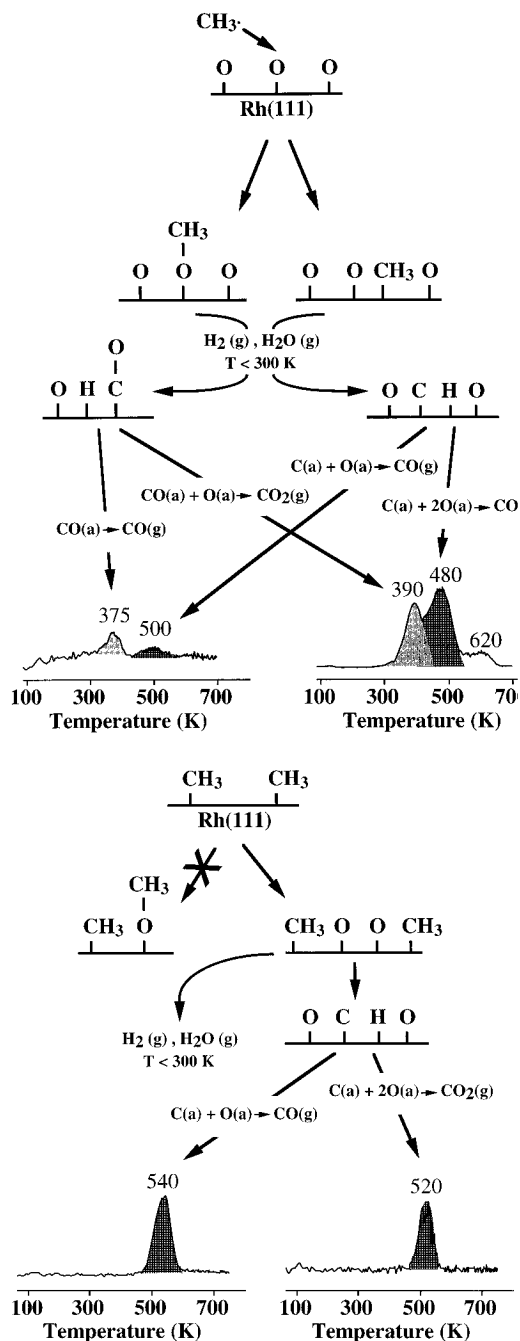


**Figure 5.** Temperature-programmed reaction data and proposed reaction scheme for (a) methoxide formed from the reaction of  $\cdot\text{CH}_3$  with oxygen-covered Rh(111) and (b) oxygen reacting with adsorbed methyl on Rh(111). The different peak temperatures for CO and  $\text{CO}_2$  evolution reflect the different mechanisms for the two reactions. (From ref 1.)

increase in the amount of alkyl iodide desorption and a corresponding decrease in the amount of reaction, with increasing oxygen coverage. Therefore, although one might intuitively expect partial oxidation to be favored at high coverages due to the increased probability of *simultaneous* I–C scission and C–O bond formation (i.e. I–C  $\rightarrow$  O), the total amount of reaction is expected to be small. Indeed, this is precisely what is observed; temperature-programmed reaction studies of  $\text{CH}_3\text{I}$  are consistent with formation of a transient methoxide species on both oxygen-covered Pd(100) and Rh(111). Unfortunately, methoxide could not be identified using vibrational

spectroscopy in either case, because it decomposes rapidly compared to the measurement time at the temperature of C–I bond dissociation.<sup>66</sup> Recently,  $\text{CH}_3\text{I}$  was found to form methoxide and formate on oxidized Cu particles supported on silica,<sup>67</sup> indicating that methyl addition to oxygen is rather general. While no experiments were specifically performed to test for differences between surface-bound and a transient methyl species, these results are generally consistent with reaction of a transient radical to form the oxygenated surface intermediate. In the case of Cu, methoxide does not decompose as readily as on Pd or Rh, probably accounting for the observation of adsorbed oxygenated species.

The addition of oxygen to transient alkyls on Rh(111) is also quite general on the basis of our investigations of other alkyl iodides.<sup>55,68</sup> Similarly, ethyl and 2-propyl iodide react via transient alkoxides which eliminate acetaldehyde and acetone, respectively, by reaction on oxygen-covered Rh(111).<sup>55</sup> A competing reaction path,  $\beta$ -hydrogen elimination, is also available to  $\text{C}_2$  and higher alkyls on oxygen-covered Rh(111).  $\beta$ -Hydrogen elimination yields ethylene, propene, and isobutene from reaction of ethyl, 2-propyl, and *tert*-butyl, respectively.<sup>55,65,68</sup> Once again, independent studies of the related alkoxides formed by decomposition of the parent alcohol on oxygen-covered Rh(111), served as the basis for these mechanistic deductions.<sup>20,64</sup> Clearly, these observations suggest that such reactions will occur for a broad range of alkyls. Therefore, a general scheme for the reactions of transient alkyl radicals with oxygen adsorbed on Rh(111) has been formulated on the basis of these experiments, as illustrated for the case of ethyl (Figure 6).

An intriguing difference exists for the reaction of *tert*-butyl iodide on Rh(111)-p( $2 \times 1$ )-O, in that gaseous *tert*-butyl alcohol evolution is observed.<sup>68</sup> As discussed above, alkoxide formation (in this case *tert*-butoxide) is proposed to occur by addition of transient *tert*-butyl radical to surface oxygen formed from C–I bond dissociation at  $\sim 260 \text{ K}$ . In fact, the *tert*-butoxide so formed remains on the surface and is readily identified using electron energy loss spectroscopy,<sup>68</sup> in direct contrast to the reactions of the primary (methyl, ethyl) or secondary (2-propyl) alkyl iodides on oxygen-covered Rh(111).<sup>54,55</sup> The markedly different behavior of the Rh-bound *tert*-butoxide is explained as follows: (1) the C–I bond is relatively weak<sup>69</sup> in the *tert*-butyl iodide, so that C–I bond breaking occurs at a lower temperature (260 K) than for 2-propyl (335 K) or ethyl iodide (375 K); and (2) the absence of C–H bonds at the 2-carbon in *tert*-butoxide imparts enhanced kinetic stability compared to 2-propoxide and ethoxide because dehydrogenation to eliminate a ketone or aldehyde is not possible in *tert*-butoxide.<sup>20</sup> The absence of this elimination pathway allows hydrogenation of *tert*-butoxide, affording gaseous *tert*-butyl alcohol. These investigations provide corroborating evidence for the proposed mechanism for reaction of other alkyl iodides on oxygen-covered surfaces and demonstrate how product distributions can be manipulated by altering the molecular structure so as to favor certain reaction paths over others. In this case, we were able to

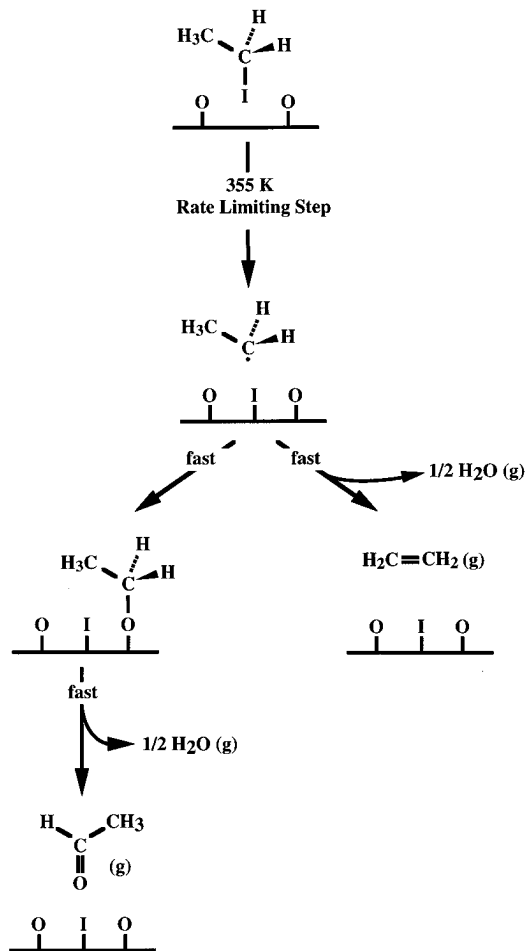


**Figure 6.** Proposed reaction scheme for ethyl iodide on  $\text{Rh}(111)\text{-p}(2\times 1)\text{-O}$ . (From ref 55.)

induce partial oxidation of the alkyl radical to the corresponding alcohol by effectively eliminating the pathway for dehydrogenation at the carbon adjacent to the oxygen by alkyl substitution.

The product distributions in the reactions of longer chain alkyl iodides depend strongly on the initial oxygen coverage. Surprisingly, the selectivity for partial oxidation increases with increasing oxygen coverage at the expense of  $\text{CO}$  and  $\text{CO}_2$  production.<sup>55,65,68</sup> For example, acetaldehyde was only formed from ethyl iodide for initial oxygen coverages above 0.25 monolayers. In addition, there is *no* detectable  $\text{CO}$  or  $\text{CO}_2$  production for ethyl or 2-propyl iodide reaction on the full-coverage  $\text{Rh}(111)\text{-p}(2\times 1)\text{-O}$  surface ( $\theta_{\text{O}} = 0.5$ ).<sup>55</sup> This surprising dependence of the product distribution on initial oxygen coverage is attributed in part to a suppression of nonselective  $\text{C-H}$  bond activation by oxygen on  $\text{Rh}(111)$ .<sup>55,56</sup> Oxygen on  $\text{Rh}(111)$  does *not* serve as a Brønsted base,<sup>70</sup> in contrast to other metals such as  $\text{Ag}$ . However,  $\text{Rh}$  itself readily activates  $\text{C-H}$  bonds. Furthermore, as shown by our investigations of  $\cdot\text{CH}_3$  and surface oxygen, the probability of forming an alkoxide via addition of an alkyl radical to oxygen increases with  $\theta_{\text{O}}$ . Taken together, these observations are consistent with an enhancement in partial oxidation at high oxygen coverage due to both the inhibition of nonselective dehydrogenation and the increased probability for oxygen addition to the transient radicals.

The reactions of transient alkyl radicals with adsorbed oxygen has broad importance in other classes of reactions as well, including thiolate desulfurization.<sup>71,72</sup> For example, 2-propyl thiolate<sup>71,72</sup> reacts similarly to 2-propyl iodide on oxygen-covered  $\text{Rh}(111)$ . The same products (acetone, propene,  $\text{H}_2\text{O}$ ,  $\text{CO}$ , and  $\text{CO}_2$ ) are formed and acetone formation is favored at high oxygen coverages in both cases. Likewise, 2-butyl thiolate reacts to form methyl ethyl ketone and butene on  $\text{Rh}(111)\text{-p}(2\times 1)\text{-O}$ .<sup>68</sup> *tert*-Butyl thiolate reacts similarly to *tert*-butyl iodide, leading to *tert*-butyl alcohol and isobutene on  $\text{Rh}(111)\text{-p}(2\times 1)\text{-O}$ .<sup>68</sup> The relative temperatures for the reactions of the various alkyl iodides and thiolates also indicate that  $\text{C-X}$  ( $\text{X}=\text{I}, \text{S}$ ) bond scission is rate limiting for high oxygen coverages, on the basis of the correlation between reaction temperature and homolytic bond strength. Accordingly, the peak temperatures for olefin elimination are 335 and 375 K for reaction of ethyl and 2-propyl iodide and their respective (gas-phase)  $\text{C-X}$  bond strengths are 54.3 and 70.5 kcal/mol, respectively.<sup>69,73</sup> The reaction temperatures for 2-propyl and 2-butyl thiolate are the same, reflecting the nearly identical  $\text{C-S}$  bond strengths of such secondary thiols. Finally, *tert*-butyl mercaptan, which has the lowest  $\text{C-S}$  bond strength, reacts at 335 K.<sup>68</sup> Hence, the variation in the alkyl substituents served both as a means of testing the generality of the reactions and probing the reaction mechanism.

Finally, the direct addition of reactive hydrocarbons to oxygen on  $\text{Rh}(111)$  also extends to methylene,  $\text{CH}_2$ , on  $\text{Rh}(111)$ .<sup>54,56,74</sup> In this case, gaseous formaldehyde is formed via the addition of a transient  $\text{CH}_2$  species formed from decomposition of either  $\text{CH}_2\text{I}_2$ <sup>74,75</sup> or partially dehydrogenated azomethane<sup>54</sup> on oxygen-covered  $\text{Rh}(111)$ . The formaldehyde production has several features that are similar to the alkyl radical reactions to form alcohols. First of all,  $\text{CH}_2$  adsorbed on clean  $\text{Rh}(111)$  does *not* form formaldehyde when oxygen is subsequently adsorbed;  $\text{CO}$  and  $\text{CO}_2$  are the only volatile carbon-containing products evolved during temperature-programmed reaction.<sup>54</sup> Secondly, the selectivity for gaseous formaldehyde production increases with increasing oxygen coverage. In addition,  $\text{C-I}$  bond dissociation is inhibited by surface oxygen such that it becomes rate-limiting for initial oxygen coverages greater than 0.25 monolayers.

Formaldehyde is also produced from  $\text{CH}_2\text{I}_2$  reaction with oxygen on  $\text{Pd}(100)$ <sup>57</sup> and from  $\text{CH}_2\text{ICl}$  on oxygen-covered  $\text{Pt}(111)$ .<sup>58</sup> On  $\text{Pd}(100)$ , photochemical decomposition of diiodomethane was used to enhance the formaldehyde yield by circumventing the barrier for  $\text{C-I}$  bond dissociation. These studies suggest that direct addition of transient methylene to surface oxygen also leads to formaldehyde production on  $\text{Pd}(100)$ . A somewhat different mechanism was proposed for the  $\text{Pt}(111)$  case: oxygen addition to either adsorbed  $\text{CH}_2$  or  $\text{CH}_2\text{Cl}$  was proposed to account for formaldehyde production.<sup>58</sup> Unfortunately, no experiments were performed to specifically distinguish between a transient methylene adding directly to surface oxygen vs oxygen insertion into a  $\text{Pt-C}$  bond.

In summary, a wealth of mechanistic information is available by relatively straightforward interpreta-

tion of spectroscopic data. However, one of the key aspects of the above analysis is the separate preparation and investigation of each of the proposed intermediates, allowing confirmation of the existence of a given species, even in the absence of sufficient sensitivity to directly detect reactive transients using vibrational spectroscopy. Similarly, the use of isotopic labeling is *vital* in order to make definitive assignments.

In the remainder of this article we will change direction slightly to discuss the additional information concerning the precise structure and bonding of surface intermediates that is available using the high-resolution and simple selection rules intrinsic to infrared reflection absorption spectroscopy. Once again, reference will be made to the observed reactivity of a given intermediate (methoxide), where appropriate, so as to correlate the as-derived structural information with the reaction products afforded.

## V. Studies of Adsorbate Structure and Bonding by Vibrational Spectroscopy

### A. Structure of Methoxide Adsorbed on Metal Surfaces

In the previous section we described the identification of a surface methoxide species formed by addition of gaseous methyl radicals to oxygen adsorbed on Rh(111) using electron energy loss spectroscopy, a technique that is particularly well suited for such "chemical fingerprinting" due to the plethora of modes that can be excited by a combination of the different scattering mechanisms. However, the relatively low resolution ( $> 30 \text{ cm}^{-1}$ ) currently attainable using such electron-based spectroscopies<sup>76</sup> and the contribution of several different scattering mechanisms effectively hinders the determination of adsorbate *structure* using this technique. Conversely, detection of a sufficient number of adsorbate modes using infrared absorption reflection spectroscopy is often a difficult task despite significant improvements in detector sensitivity. For example, all but the most intense vibrational modes of surface alkyl species such as  $\text{CH}_x$  ( $x = 1, 2, 3$ ) are generally beyond the detection limit, so that even identification of these adsorbates is difficult using surface infrared spectroscopy. However, for higher hydrocarbons ( $\text{C}_2$  and above) the number density of oscillators is increased for the same surface coverage, so that multiple modes may be observed. Alternatively, if the adsorbate possesses a large permanent dipole moment, the dynamic dipole moments associated with the motion of neighboring functional groups (e.g. the methyl group in  $\text{CH}_3\text{O}^-$ ) may be significantly enhanced. Indeed, it is in part for this latter reason that considerable attention has been devoted to the determination of the structure of adsorbed methoxide; it represents one of the simplest polyatomic adsorbates for which the majority of the vibrational modes are generally detectable. As such, these studies have essentially been regarded by the surface science community as a test of the utility of surface infrared spectroscopy for probing the adsorbate overlayers. Despite this interest, there has been considerable debate over the interpretation of the surface infrared

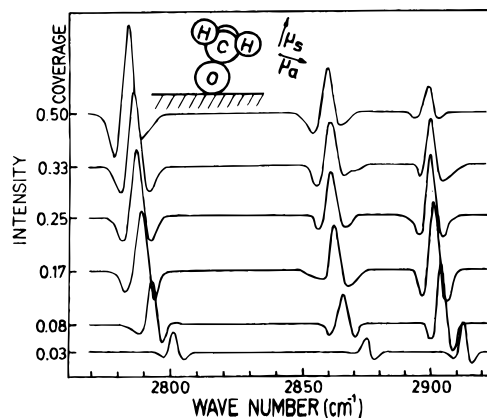


**Figure 7.** Infrared spectra of the C–H stretching region of methoxide on Cu(100), as a function of coverage. (Taken from Ryberg, ref 84.)

spectrum of methoxide adsorbed on metal surfaces. Specifically, the focus of the controversy is the assignment of the  $2700\text{--}3100 \text{ cm}^{-1}$  region, over which frequency range the C–H stretching vibrations are known to occur. Importantly, these modes contain vital symmetry information and are readily observable using a standard MCT (mercury–cadmium–telluride) detector. In contrast, the lower frequency methyl bending and rocking modes, which are also symmetry sensitive, typically have much smaller dynamic dipole moments so that only the symmetric methyl deformation is observable on many surfaces. In addition, orientational analyses based on the absolute absorbance of this mode for a given adsorbate coverage are largely meaningless, since one cannot *a priori* predict how the intrinsic intensity of this mode is modified by the adsorption process. Consequently, we will focus predominantly on the interpretation of the C–H stretching region in this discussion, but will also refer to data obtained in the  $1000\text{--}1450 \text{ cm}^{-1}$  region where available, in order to verify that a self-consistent picture can be obtained by careful design of the experiment.

The earliest vibrational studies of an adsorbed methoxide species were reported over 15 years ago by Sexton<sup>77</sup> and Ibach et al.<sup>78</sup> Both of these studies and, indeed, over half of all the studies of alkoxides to date, utilized electron energy loss spectroscopy as the primary surface probe.<sup>21,22,79–83</sup> However, for the reasons discussed above, the structural assignments in these studies are often ambiguous. Therefore, we will not discuss this work further and will focus entirely on the use of infrared reflection absorption spectroscopy in the remainder of this section.

The first reported infrared study of methoxide on a single-crystal metal surface was an investigation on Cu(100) by Ryberg,<sup>84</sup> over a decade ago. In that study, three absorption bands were observed in the  $2700\text{--}3100 \text{ cm}^{-1}$  region at all coverages studied (Figure 7). The most intense feature at  $2787 \text{ cm}^{-1}$  was assigned to the symmetric C–H stretching mode; representing a downshift of over  $60 \text{ cm}^{-1}$  from the known frequency of this mode in the gas phase. Furthermore, the remaining bands at  $2861$  and  $2901 \text{ cm}^{-1}$  were assigned to the two components of the asymmetric stretching mode which, although surface-dipole forbidden for a  $\text{C}_{3v}$  adsorbate symmetry ( $E$

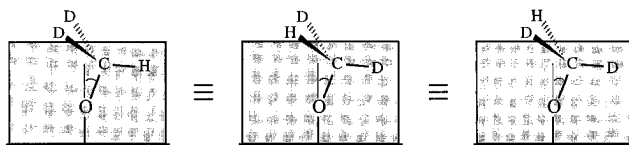
**Table 1. Relevant Part of the Correlation Table for the Irreducible Representations of the Symmetry Groups That May Apply to the Adsorbed Methoxide,  $\text{CH}_3\text{O}^-$** <sup>a</sup>

mode	adsorbate symmetry		
	$C_{3v}$	$C_s$	$C_1$
$\nu(\text{C}-\text{O})$			
$\delta_a(\text{CH}_3)$	<b>A<sub>1</sub></b>	<b>A'</b>	<b>A</b>
$\nu_s(\text{C}-\text{H})$			
$\rho(\text{CH}_3)$			
$\delta_s(\text{CH}_3)$	<b>E</b>	<b>A' + A''</b>	<b>A + A</b>
$\nu_a(\text{C}-\text{H})$			

<sup>a</sup> Modes that transform as the representations indicated in bold are surface-dipole allowed.

representation), become allowed if the adsorbate symmetry is lowered to  $C_1$  (Table 1). Consequently, it was suggested that methoxide adsorbs with the C–O axis tilted with respect to the surface normal on Cu(100), although a  $C_s$  adsorbate symmetry group was (incorrectly) suggested. This tilted geometry was contradicted by ultraviolet photoemission studies by Stöhr et al., which were interpreted in terms of an upright structure.<sup>85</sup> Before proceeding to detail more recent infrared studies of methoxide on other surfaces, it is useful to note that in all of these subsequent studies the essential features of the data obtained for  $\text{CH}_3\text{O}$  adsorbed on Cu(100) are reproduced, although additional features are also observed on some surfaces.

Two years later, Chesters and McCash used infrared spectroscopy to study the adsorption of methoxide on Cu(111)<sup>86</sup> for which a similar spectral signature was observed in the C–H stretching region to that reported for Cu(100). However, by comparison of data obtained using  $\text{CH}_3\text{O}^-$  and  $\text{CD}_3\text{O}^-$ , they proposed that the highest frequency mode observed at  $2916\text{ cm}^{-1}$  was due to an overtone of a methyl deformation mode in Fermi resonance with the symmetric C–H stretching fundamental at  $2818\text{ cm}^{-1}$ , in contrast to Ryberg's assignment to  $\nu_a(\text{C}-\text{H})$ , suggestive of a  $C_{3v}$  adsorbate symmetry on this surface. Indeed, some additional support for this assignment was provided by reference to methoxide-osmium cluster data. However, these assignments were sufficiently controversial that Zenobi et al. favored those of Ryberg when assigning the spectrum of methoxide on Ni(111).<sup>87</sup> Similarly, Dastoor et al. also assigned two modes at  $2908$  and  $2920\text{ cm}^{-1}$  observed for  $\text{CH}_3\text{O}_{(a)}$  on Ni(110) to the in-plane asymmetric C–H stretching modes of two  $C_s$  symmetry methoxide species.<sup>88</sup> The latter assignments were justified by the coincident observation of a feature at  $1154\text{ cm}^{-1}$  that can be unambiguously attributed to a component of the methyl rocking mode that, once again, only becomes allowed for an adsorbate symmetry lower than  $C_{3v}$ . Thus, it began to appear that a general consensus of opinion had been reached and the overlayer structure solved. Unfortunately, parallel studies of methoxide adsorbed on both Cu(111)<sup>79</sup> and Ni(111),<sup>89</sup> using photoemission and photoelectron diffraction, respectively, concluded that in both cases the C–O axis was perpendicular to the surface plane, indicative of a  $C_{3v}$  adsorbate symmetry. Indeed, this disparity between the con-

**Figure 8.** Schematic diagram showing the “equivalence” of the C–H(D) coordinates in selectively isotopically labeled methoxide.

clusions of infrared studies and those of other, more established structural probes, led some workers to suggest that surface infrared spectroscopy was of limited utility for structural analyses.

Motivated by an interest in using vibrational spectroscopy as a structural tool, we decided to adopt an approach pioneered by McKean<sup>90–93</sup> for methyl-containing species in the gas phase: that of selective isotopic labeling.<sup>23,94,95</sup> In short, the essence of this approach is to use  $\text{CHD}_2\text{O}^-$  to effectively remove the contribution of the Fermi resonances which are known to be prevalent in gaseous methyl-containing species (including methanol) while at the same time revealing C–H bond inequivalency and, therefore, the molecular symmetry. The uncoupling of the C–H stretching modes from the overtones of the bending modes results from the fact that the highest frequency bending mode in the selectively labeled molecule is now at  $\sim 1350\text{ cm}^{-1}$ ,  $\sim 100\text{--}150\text{ cm}^{-1}$  lower than for  $\text{CH}_3\text{O}^-$ , so that the overtone modes are no longer near-degenerate with the C–H stretching fundamentals and the coupling is consequently negligible. Notably, there is still the potential for Fermi resonance in adsorbed  $\text{CD}_3\text{O}^-$  because both the  $\text{CD}_3$  deformations and stretches shift to lower frequency. In addition, the first overtones of the methyl rocking modes, as well as the C–O stretching vibration, may also contribute intensity in the nominal C–D stretching region ( $1950\text{--}2250\text{ cm}^{-1}$ ), effectively hindering conclusive assignment of the vibrational modes using the perdeuterated molecule.

The second advantage of the *selective* isotopic labeling approach is that the C–H coordinate is isolated (or uncoupled) from the two C–D coordinates, so that the number of distinct C–H modes observed directly reveals the adsorbate symmetry, in the following way: all coordinates are necessarily equivalent for  $C_{3v}$  symmetry so that only a single C–H mode should be observed in this case. In contrast, there are two inequivalent positions for  $C_s$  symmetry due to motion in and out of the mirror plane. Finally, all coordinates are inequivalent for  $C_1$  adsorbate symmetry, so that three distinct modes will be observed. Note: the use of deuterium substitution (as opposed to a chemically distinct species) ensures that an ensemble of methoxide species will contain all possible (static) C–H bond dispositions, as shown in Figure 8. In this way, the single C–H coordinate probes the full symmetry of the adsorbate.

The results of a study of  $\text{CHD}_2\text{O}^-$  and  $\text{CH}_3\text{O}^-$  adsorbed on Mo(110) are shown in Figures 9–11. Representative C–H spectra for a low coverage ( $<0.17\text{ ML}$ ) of  $\text{CHD}_2\text{O}^-$  (Figure 9a) and  $\text{CH}_3\text{O}^-$  (Figure 10a) reveal one and three distinct modes, respectively. By the preceding analysis, one can immediately conclude that the presence of only a single C–H stretch for the labeled species at low

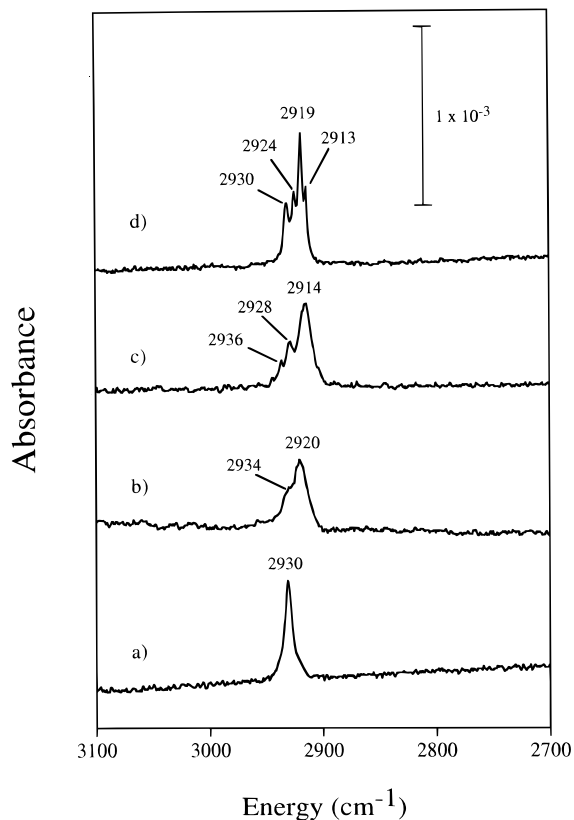


**Figure 9.** Infrared spectra of the C–H stretching region of  $\text{CHD}_2\text{O}^-$  on Mo(110) at coverages of (a) 0.17 ML, (b) 0.19 ML, (c) 0.23 ML, (d) 0.25 ML (saturation). (From ref 23.)

coverage indicates that the symmetry must be  $C_{3v}$ ; that is, the C–O bond is normal to the molybdenum surface.<sup>96</sup> Consequently, only one of the bands in the spectrum of  $\text{CH}_3\text{O}^-$  can be due to a C–H stretching fundamental, that at  $2811\text{ cm}^{-1}$ . The other two features at  $2868$  and  $2916\text{ cm}^{-1}$  must be due to overtones of methyl deformations, gaining intensity by Fermi resonance with the  $\nu_s(\text{C–H})$  mode. Indeed, for  $C_{3v}$  symmetry two such overtones transform as the totally symmetric representation and can therefore mix with  $\nu_s(\text{C–H})$ . Further support for this assignment is obtained by inspection of the low-frequency region of the infrared spectrum of  $\text{CH}_3\text{O}^-$  (Figure 11a). Notably, only the symmetric methyl deformation is observed which is totally symmetric for  $C_{3v}$  symmetry, whereas the asymmetric deformations and methyl rocking modes, both of which transform as the doubly degenerate  $E$  representation under  $C_{3v}$ , are absent at low methoxide coverage.

The coverage dependence of the features is also a rich source of additional information (Figures 10 and 11). A pronounced shoulder is apparent at  $2934\text{ cm}^{-1}$  in the spectrum of  $0.19\text{ ML}$  of  $\text{CHD}_2\text{O}^-$ , indicative of a second, nonequivalent C–H coordinate and thus a lowering of the adsorbate symmetry to  $C_s$ , as the coverage is increased from  $0.17\text{ ML}$ . In addition, new features are observed at  $1150$ ,  $1445$ , and  $2960\text{ cm}^{-1}$  in the spectrum of  $\text{CH}_3\text{O}^-$ , which can be assigned to  $\rho(\text{CH}_3)$ ,  $\delta_a(\text{CH}_3)$ , and  $\nu_a(\text{C–H})$ , respectively, all of which become surface dipole allowed under  $C_s$  symmetry (Table 1). Interestingly, the position of the  $\nu_a(\text{C–H})$  band is precisely in accordance with reference data, allowing for a similar downshift as is

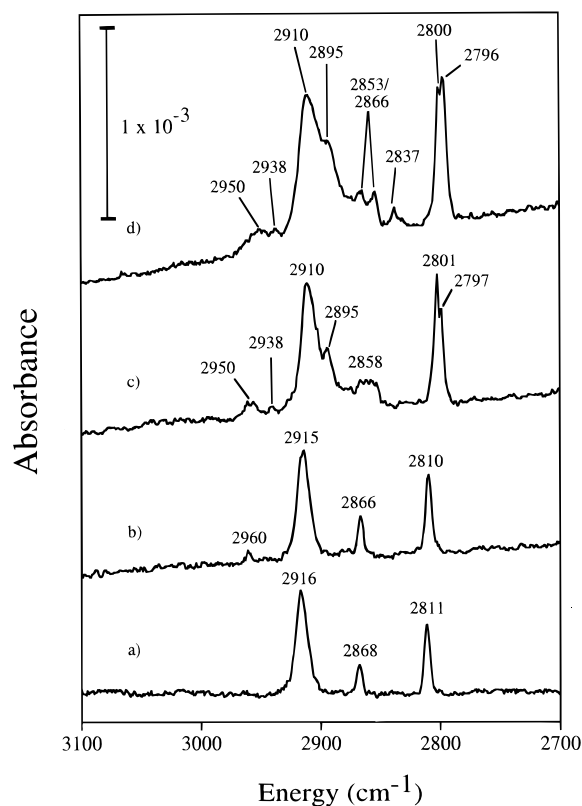


**Figure 10.** Infrared spectra of the C–H stretching region of  $\text{CH}_3\text{O}^-$  on Mo(110) at coverages of (a) 0.17 ML, (b) 0.19 ML, (c) 0.23 ML, and (d) 0.25 ML (saturation). (From ref 23.)

observed for  $\nu_s(\text{C–H})$ , upon adsorption (Table 2). Finally, as the coverage is increased to saturation ( $0.25\text{ ML}$ ), two  $C_s$  symmetry methoxide species are observed, based on the doubling of all the bands observed at lower coverage and the existence of two C–O stretch modes over this coverage range.

There are several important conclusions from this work:

(i) Fermi resonances dominate the  $2700\text{--}3100\text{ cm}^{-1}$  region of the infrared spectrum of both  $C_{3v}$  and  $C_s$  symmetry  $\text{CH}_3\text{O}^-$  species adsorbed on Mo(110), as is the case for homogeneous methyl-containing species. Furthermore, selective isotopic labeling is a valuable tool in the surface infrared spectroscopist's arsenal (see below).

(ii) On the basis of the excellent correspondence between the data for Mo(110) and that obtained on all other surfaces studied to date, these assignments should be generally applicable to methoxide adsorbed on (metal) surfaces. Indeed, if previous spectra are so assigned, the disparity between the structures predicted by infrared spectroscopy and other structural probes for methoxide on Cu(100), Cu(111), and Ni(111) is removed. Interestingly, our conclusions concerning the generality of the above assignments of the C–H stretching region of methoxide were recently duplicated in a study of  $\text{CH}_3\text{O}^-$  on oxygen-covered Ag(111).<sup>97</sup> However, the vibrational assignments in that study were made by reference to data obtained using the perdeuterated ( $\text{CD}_3\text{O}^-$ ) species and therefore relied on plausibility arguments, based on spectral line widths. In addition, although the authors demonstrated the existence of Fermi reso-

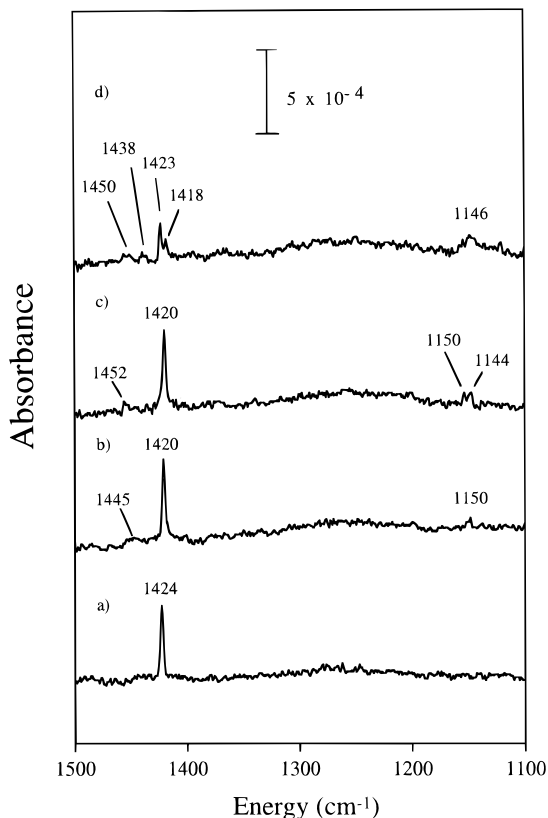


**Figure 11.** Infrared spectra of the CH<sub>3</sub> bending and rocking modes of CH<sub>3</sub>O<sup>-</sup> on Mo(110) at coverages of (a) 0.17 ML, (b) 0.19 ML, (c) 0.23 ML, and (d) 0.25 ML (saturation). (From ref 23.)

nances in adsorbed methoxide, the absence of the asymmetric C–H stretching mode (indicative of symmetry lower than  $C_{3v}$ ) cannot be conclusively inferred from the data presented,<sup>98</sup> making the structural assignment slightly tenuous.

(iii) If data obtained using both infrared and electron energy loss spectroscopy is compared, an interesting disparity in the intensity distribution in the C–H stretching region is immediately apparent (Figure 12). There is a pronounced maximum at  $\sim 2920$  cm<sup>-1</sup> with considerably less intensity at 2800 cm<sup>-1</sup> in the electron energy loss spectrum. This is in stark contrast to the infrared data, which shows similar (peak) intensity in these two regions. The origin of this discrepancy is elucidated by investigation of the intensity distribution in the 2700–2900 cm<sup>-1</sup> region, as a function of incident electron energy.

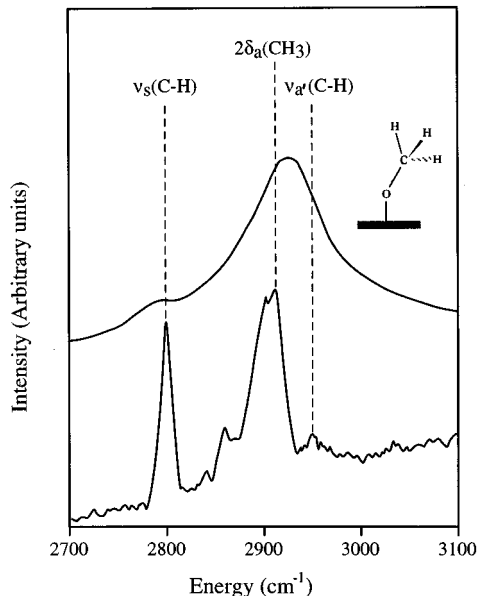


**Figure 12.** (a) Comparison of the spectra obtained for the C–H stretching region of 0.25 ML of CH<sub>3</sub>O–Mo(110) using infrared (bottom) and electron energy loss (top) spectroscopies (3 eV primary electron energy). Note: the infrared data were collected at low (4 cm<sup>-1</sup>) resolution and only averaged over 300 scans, resulting in a marked difference in spectral “quality” between this data and the higher resolution (2 cm<sup>-1</sup>), extensively signal-averaged (>1000 scans) spectrum presented in Figure 10d, for the same overlayer.

The loss at 2920 cm<sup>-1</sup> is an extremely sensitive function of energy, indicative of a substantial resonance scattering contribution, so that the assumption that dipole-scattering predominates for on-specular data collection is clearly *not* valid in this instance. Consequently, structural assignments cannot be made by simple application of the surface dipole selection rule to the losses associated with the C–H stretching modes.

(iv) The last, but probably the most pertinent point, is that there is a wealth of homogeneous and organometallic reference data as well as novel methodologies in the literature that are potentially invaluable to the surface science community, but which are all too often overlooked.

Now, the question naturally arises as to how generally applicable the technique of selective isotopic labeling is to the study of adsorbate systems. We conclude this section by presenting data we have

**Table 2. Vibrational Assignments for the C–H Stretching Region of Methoxide Adsorbed on Various Metal Surfaces, Compared to Matrix-Isolated Methanol<sup>a</sup>**

Mo(110) <sup>94</sup>	Cu(100) <sup>84</sup>	Cu(111) <sup>86</sup>	Ni(111) <sup>87</sup>	methanol <sup>118</sup>	assignment
<b>2960</b>				3005	$\nu_a(\text{C-H})$
2915	2901	2918	2921	2956	$2\delta_a(\text{CH}_3)$
2866	2861	2882	2878		$2\delta_s(\text{CH}_3)$
2810	2787	2818	2817	2847	$\nu_s(\text{C-H})$
<b>1445</b>				1473	$\delta_a(\text{CH}_3)$
1420		1435		1451	$\delta_s(\text{CH}_3)$
<b>1150</b>				1155	$\rho(\text{CH}_3)$
1014		1036	1027	1033	$\nu(\text{C-O})$

<sup>a</sup> All values are in wave numbers (cm<sup>-1</sup>). Data for 0.19 ML of methoxide on Mo(110) ( $C_s$  symmetry) have been used for comparison with the isolated molecule; the additional modes that are present at this coverage due to the lowering of the symmetry from  $C_{3v}$  at 0.17 ML are highlighted in bold. The remaining modes are observed at essentially the same frequency for the two adsorbate symmetries/coverages and therefore can be compared to the data obtained for (proposed)  $C_{3v}$  symmetry species on the other surfaces surveyed.

recently acquired for 2-propoxide,<sup>95,99</sup> which also exhibits C–H mode inequivalency due to a  $C_s$  adsorbate symmetry. These experiments show that the approach developed for adsorbed methoxide can be applied to more complex systems. From a practical standpoint there are two essential requirements: (i) it must be possible to isolate a C–H coordinate, and (ii) there must be sufficient sensitivity of this coordinate to the local environment to permit resolution of any asymmetry by surface infrared spectroscopy. Generally, it is desirable that the isolated C–H coordinate be proximal to a functional group with a highly localized or structured charge distribution so that (a) there is not free rotation in the adsorbate species, which would result in a single averaged spectral feature regardless of symmetry, and (b) the inequivalent coordinates are separated by  $>5\text{ cm}^{-1}$  and can therefore be readily resolved. Importantly, McKean has demonstrated that these criterion are met for a variety of gaseous and condensed phase  $C_xH_yX^-$  containing species, where  $X = O, N,$  and  $F$ .<sup>90–93</sup>

The data reproduced in Figure 13 show the coverage dependence of the C–H stretching modes of the selectively labeled,  $(CD_3)_2C(H)O^-$  isotopomer of 2-propoxide adsorbed on Mo(110).<sup>99</sup> The selection of this particular isotopic species was made by reference to the normal-mode frequencies of the condensed-phase molecule; the overtone of the highest frequency bending mode is effectively uncoupled from the C–H stretching mode by deuteration of all of the methyl hydrogens, as was demonstrated for  $CHD_2O^-$ . However, there is an important difference between the two cases; namely that there is inherent inequivalence about the 1-carbon position in 2-propoxide due to the presence of the two C–C coordinates. The reason that this is potentially significant is that the molecule could, in principle, adsorb with a preferential (fixed) disposition of the C–C coordinates with respect to the surface, so that the C–H coordinate was no longer able to probe the various angular positions about the C–O bond. This would result in the observation of a single C–H stretch mode, independent of the adsorbate symmetry, but simple inspection of the infrared spectra obtained for 2-propoxide reveals that this is not the case; two distinct C–H modes are observed over the entire coverage range studied for a single C–O bond environment.<sup>100</sup> From this observation alone, one can immediately conclude that 2-propoxide adsorbs with  $C_s$  symmetry on Mo(110). Furthermore, information about the *rotational* freedom in the molecule is also contained in the spectra, as follows: there are two possible explanations for the fact that each of the two coordinates can be probed in this experiment (Figure 14). The first is that there is no rotational freedom about the C–O bond in the adsorbate, but there are two stable (fixed) configurations; e.g. with the C–H oriented toward, or away from, the molybdenum surface. The second possibility is that there is hindered rotation about the C–O bond, so that the C–H coordinate can exist in each of the stable configurations in turn. On first consideration, it may appear that it is virtually impossible to distinguish between the two scenarios. However, a closer inspection

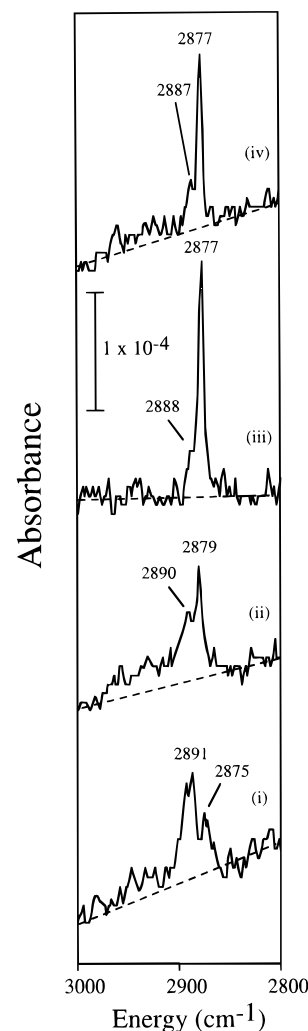


**Figure 13.** Infrared spectra of the C–H stretching region of  $(CD_3)_2C(H)O^-$  on Mo(110) at coverages of (i) 0.12 ML, (ii) 0.15 ML, (iii) 0.20 ML, and (iv) 0.25 ML (saturation). The dashed line is drawn to illustrate the broad-band absorption seen between 2900–2970  $cm^{-1}$ . (From ref 99.)

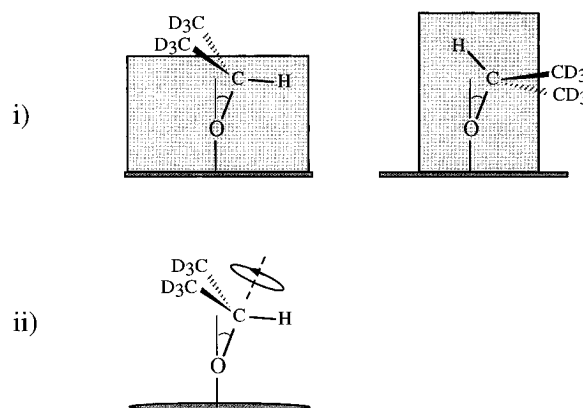


**Figure 14.** Schematic showing the two canonical adsorbate-substrate interactions for  $(CD_3)_2C(H)O^-$ -Mo(110): (i) preferential adsorption of the C–H bond and (ii) hindered rotation about the C–O bond.

tion of the data reveals the presence of a broad-band absorption at higher frequency than the two discrete states, suggestive of the existence of less stable intermediate configurations of the adsorbate-surface complex, as would be expected if there were a hindered rotational motion about the C–O bond. Furthermore, the energies of the two fixed orienta-



tions that would still retain the mirror plane of the molecule are probably the most different of any two possible orientations, since they represent the extremes of surface-methyl interactions (Figure 14). Hence, it is highly improbable that a mixture of these two fixed orientations would be favored. Consequently, we favor the model in which there is hindered rotation about the C–O bond. Clearly, detailed calculations of the relative stability of different azimuthal orientations at different adsorbate coverages would be invaluable to strengthen these arguments.

In summary, these studies have demonstrated the potential of selective isotopic labeling, in combination with surface infrared spectroscopy, as a structural probe of complex overlayers and will hopefully serve to motivate future theoretical and experimental investigations of the internal dynamic motion of adsorbates.

### B. Determination of C–O Bond Strength in Adsorbed Methoxide by Surface Overtone Spectroscopy

Understanding the catalytic activity of transition metals is one of the most important driving forces behind studies of adsorbates on single-crystal metal surfaces. Particularly, delineation of the mechanism of facile, heterogeneous C–X bond scission (e.g. X = O, S, F, Cl, Br, I, H) is of great importance in such technologically diverse areas as hydrodesulfurization, hydrocarbon cracking, and diamond atomic layer epitaxy, as described in the introduction. However, in spite of the proposed importance of bond weakening upon adsorption, there exist only a few direct observations of surface-induced bond weakening of adsorbed species that consider the possibility that the shape of the intramolecular potential is changed upon adsorption. Previously, bond weakening has only been inferred by indirect means from kinetic studies or surface-induced shifts in the *fundamental* vibrational modes. The utility of these techniques is severely limited by the inherent assumptions; i.e. in the case of kinetic studies, the dissociation energy of a given adsorbate bond is estimated from the activation energy for gaseous product evolution. However, this requires that a reaction pathway exists for which the activation energy is *solely* a function of the relevant bond scission kinetics, which is rarely the case. In addition, further assumptions are usually necessary concerning, for example, the pumping speed, preexponential factor, and order of the reaction. Similarly, there is no direct theoretical relation between the *fundamental* frequency of a vibrational mode and the dissociation energy of the related bonds; in fact, they are independent parameters in the harmonic limit. Despite this, a close (linear) correlation is often observed in the gas phase, which has led to the derivation of a number of empirical formulae (e.g. Badger's rule) that relate experimental observables with quantities of interest such as the force constant, dissociation energy, bond order, and the equilibrium bond length.<sup>37</sup> Furthermore, the remarkable success of these rules for gaseous and metal carbonyl species has led many surface scientists to believe that a similar correlation may also

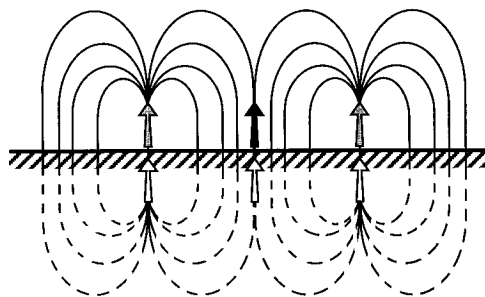


**Figure 15.** Schematic depiction of the influence of the dipole field of neighboring adsorbates on an identical dipole's local environment causing depolarization and an increase in the observed frequency of the relevant vibrational mode.

exist for adsorbates. In contrast, no significant correlation has been observed in the heterogeneous systems studied to date, although the database is still rather small. However, if indeed there are no analogous laws for adsorbates on extended surfaces, it is not difficult to see why this might be the case, by reference to the existing literature on the effect of intermolecular coupling on the observed vibrational frequency. Specifically, it has been shown by many experimental and theoretical analyses that *dynamic* dipole–dipole coupling between adsorbates can lead to enormous ( $\sim 50\text{--}100\text{ cm}^{-1}$ ) shifts in the *observed* frequency.<sup>101</sup> Importantly, this dynamic coupling is an artifact of the simultaneous excitation of multiple adsorbate species by the external probe, which results in the perturbation of a given oscillator by the dynamic dipole moments of other (excited) oscillators, as depicted in Figure 15. The net effect on a perpendicular dipole is 2-fold: firstly, each excited species experiences an additional restoring force to the dynamic dipole field of other oscillators, and secondly, if the overlayer is inhomogeneous, then the higher frequency oscillators effectively screen the field of the lower frequency ones, leading to a net transfer of intensity to the high-frequency species.<sup>102</sup> The combined effect is to (i) shift the observed frequency of all the constituent (coupled) species to higher energy, and then (ii) to shift the absorption maximum from the mean frequency to the highest frequency in the band of states. Now, the key point is that this shift is *unrelated* to the observed thermal decomposition kinetics, as it is only present during vibrational excitation of the overlayer. Therefore, if this effect dominates the observed shift upon adsorption, the fundamental frequency will bear no simple relation to the thermal dissociation energy. However, if this dynamic dipole coupling could be quantified, the possibility remains that a surface analog of Badger's rule may exist. In fact, as we discuss below, no such correlation exists, even after the appropriate correction is applied to the experimental data, for the limited data set available.

The use of overtone spectroscopy to study bond energies is well established in the gas phase.<sup>103</sup> Similarly, a number of overtone studies of atomic and diatomic adsorbates have been reported in the literature, using the enhanced sensitivity of electron energy loss spectroscopy, described earlier.<sup>104–114</sup> However, no account was taken of the effect of dynamic intermolecular coupling in the majority of

these studies, so that the derived anharmonicities and adsorbate bond energies are difficult to interpret. Indeed, the low resolution inherent to the technique, coupled with prevalence of multiple loss features that overlap the overtone band, effectively prevents such a quantitative analysis. For this reason, the high resolution attainable using infrared spectroscopy makes it well suited to the study of adsorbate overtones. However, the infrared intensity of these overtone transitions is generally very low (<1%) compared to that of the fundamental, so that one is effectively limited to the study of vibrational modes that exhibit very intense dipole moments, such as those with carbon–oxygen bond, which will necessarily exhibit strong dipole–dipole coupling.

As a result of these limitations, there has only been one previous report of the observation of a first overtone of an adsorbate mode using surface infrared spectroscopy. In that study of the C–O stretching mode of methoxide adsorbed on Ni(111),<sup>87</sup> isotopic dilution studies were performed to quantify the effect of dipole–dipole coupling on the observed fundamental frequency. The rationale behind this methodology is that if an overlayer of, for example, CH<sub>3</sub>O– is successively diluted with a suitable isotopomer that possesses a distinctly different C–O stretching frequency, the dynamic interadsorbate coupling is effectively minimized or completely removed by extrapolation to the infinite dilution limit.<sup>102</sup> Importantly, this approach does not affect the *chemical* state of the system, as would almost certainly be the case if the adsorbate coverage were systematically lowered instead. Unfortunately, the effect of this coupling on the observed overtone frequency was not experimentally accessible, so that a theoretical approach known as the coherent potential approximation (CPA) was employed.<sup>102</sup> Interestingly, the conclusion of this study was that the calculated anharmonicity of 8.5 cm<sup>-1</sup> was actually ~40% lower than the corresponding value in gaseous methanol, suggestive of an *increase* in the C–O bond strength upon adsorption. This observation is generally consistent with the observed thermal chemistry of this species on Ni(111), which proceeds via C–H bond scission, leaving the C–O bond intact.

In contrast, the carbon-oxygen bond of methoxide on Mo(110) is facily cleaved at 300 K, so that the adsorption-induced perturbation of the C–O bond potential is expected to be very pronounced.<sup>23,115</sup> Importantly, no ordered overlayer structures were observed for any coverage of methoxide on this surface, so that the applicability of the coherent potential approximation is questionable. Therefore, we have undertaken a comprehensive experimental study of this system, involving analyses of the frequency shifts of both  $\nu(\text{C-O})$  and the  $2\nu(\text{C-O})$  as a function of isotopic dilution and coverage.<sup>115</sup>

Surface infrared spectra of the  $\nu(\text{C-O})$  and the  $2\nu(\text{C-O})$  modes of different coverages of methoxide adsorbed on Mo(110) are shown in Figure 16. In addition, the results of isotopic dilution studies for each coverage are shown in Figure 17. The strong coupling between adsorbate molecules is apparent by inspection of the 10–18 cm<sup>-1</sup> dipole–dipole shift observed for all three coverages studied. Conse-

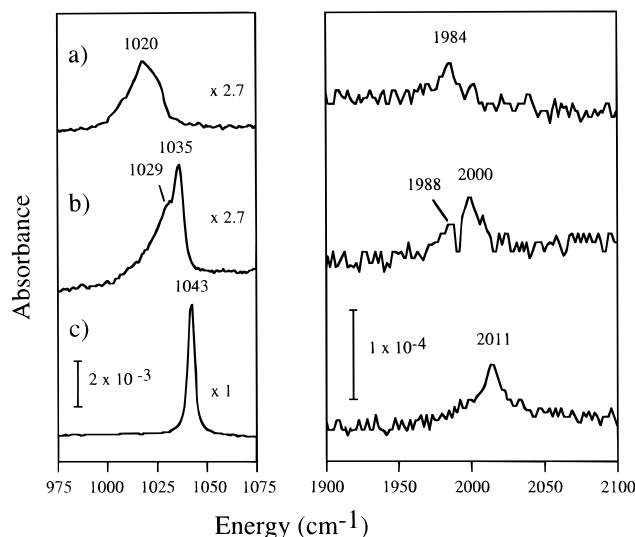


**Figure 16.** Infrared spectra of the  $\nu(\text{C-O})$  and  $2\nu(\text{C-O})$  regions for methoxide on Mo(110) at coverages corresponding to (a) 0.20 ML, (b) 0.22 ML, and (c) 0.25 ML. (From ref 115.)

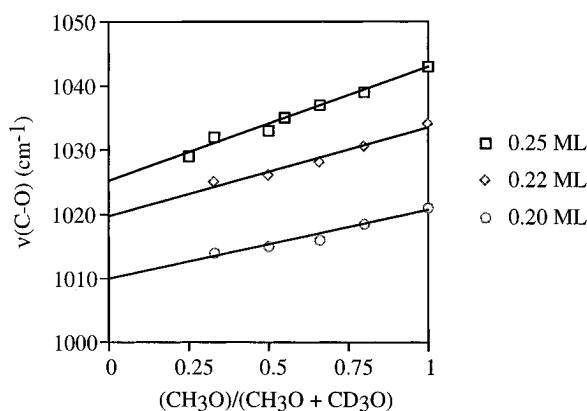


**Figure 17.** Plot of the observed frequency of the C–O stretching mode, as a function of isotopic dilution of CH<sub>3</sub>O– with CD<sub>3</sub>O–. (From ref 115.)

quently, the C–O modes must be interpreted in terms of adsorbate phonons, in accordance with the work of Richter et al.<sup>104</sup> and Guyot-Sionnest.<sup>105</sup> In this formalism, multiple phonon excitations are possible, due to the coherent motion of the adsorbate species that constitute the overlayer, with the result that the overtone states that exist in the localized description may now become embedded in the  $n$ -phonon bands. This can be visualized as follows: in the presence of strong intermolecular coupling the overtone excitation does not remain “bound” to a single adsorbate species, but drifts out into the two-phonon band, so that the observed spectra are no longer sensitive to the details of the intramolecular potential. However, there is an important exception: if the mechanical anharmonicity is sufficiently large, a so-called “two-phonon bound state” can become detached from the two-phonon band (Figure 18). Importantly, in this state the excitation is only delocalized over a few neighboring adsorbate bonds so that the observed frequency is once again sensitive to the anharmonicity of the *intramolecular* potential. Therefore, if it is possible to definitively identify this state, information about the adsorbate bond energy can indeed be obtained. Fortunately, a two-phonon

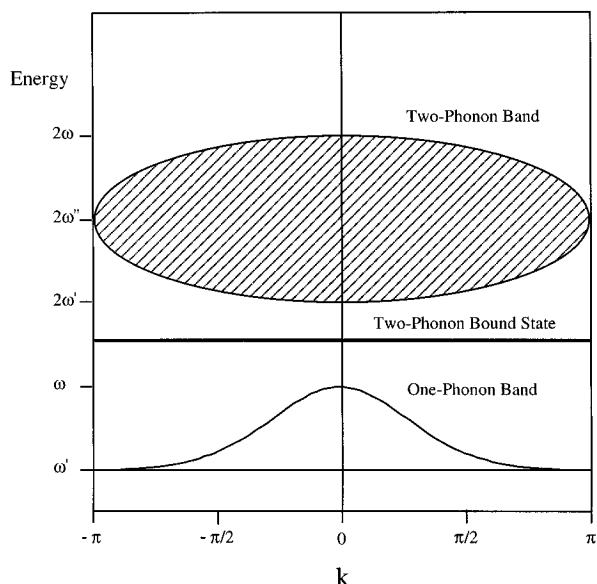


**Figure 18.** Conceptual illustration of the one- and two-phonon bands of a (coupled) adsorbate overlayer and the existence of a two-phonon bound state which exhibits negligible dispersion in the presence of significant mechanical anharmonicity. (After Richter et al., ref 104.)

bound state has a characteristic spectral signature, consisting of an absorption maximum well below the minimum energy of the  $2\omega$  band, which exhibits only very weak dispersion. Indeed, it has been shown by Richter et al.<sup>104</sup> that essentially all the dispersion exhibited by this state arises from the interaction with the two-phonon continuum, so that the *absence* of any appreciable dispersion confirms that no such mixing exists and the excitation is localized.

This is precisely what is observed for methoxide on Mo(110). The minimum of the two-phonon band can be estimated by reference to the isotopic dilution data, since it has previously been shown for CO adsorbed on Cu(100) that the measured frequency at the isotopic dilution limit is in good agreement with that observed at the edge of the adsorbate Brillouin zone ( $k = \pm\pi$ ).<sup>102,116</sup> Now, the  $2\omega$  band minimum (at  $k = 0$ ) is given by sum of  $\omega(k = +\pi)$  and  $\omega(k = -\pi)$ , which can be approximated by twice the dilution limit frequency.<sup>117</sup> In this way, we find that  $2\omega(k = 0)$  occurs at 2020 and 2050  $\text{cm}^{-1}$  for the 0.20 and 0.25 ML overlayers, respectively, so that the features observed at 1984 and 2011  $\text{cm}^{-1}$  in the two cases are more than 35  $\text{cm}^{-1}$  below this energy. The same is also true for the two species that form the 0.22 ML overlayer. Furthermore, we observed no dispersion of these states even half way to the edge of the Brillouin zone (beyond which the intensity became vanishingly small). These data allow a definitive assignment of these features as two-phonon bound states which, by definition, are sensitive to the intramolecular anharmonicity, as discussed above. As a result we find that the C–O bond in methoxide on Mo(110) exhibits an anharmonic shift of  $39 \pm 3 \text{ cm}^{-1}$  at all three coverages, which is more than three times that in gaseous methanol. If a Morse potential is used to estimate the bond dissociation energy, a value of  $\sim 40 \text{ kcal/mol}$  is obtained, representing a  $>70\%$  reduction from the gas-phase species,<sup>118</sup> consistent

with the facile C–O bond scission observed on this surface.

There are several important conclusions that result from these studies. Firstly, it appears that the reorientation of the methoxide species observed over this coverage range (see section V.A) has no discernable effect on the C–O bond anharmonicity. Interestingly, this finding is in complete agreement with the observed reactivity of methoxide, in that the temperature at which decomposition (via C–O bond scission) occurs is essentially invariant with coverage.<sup>23</sup> The absence of a significant effect of C–O–Mo bond angle on the bond strength is, however, somewhat surprising and may indicate that the change in adsorbate structure over this coverage range is rather small. Indeed, quantitative determination of the tilt angle by infrared spectroscopy remains problematic given that the intrinsic dipole moments of the adsorbate are *not* known and cannot reliably be estimated from the condensed molecule, since adsorption of methoxide on Mo(110) clearly results in significant changes in the intramolecular modes.<sup>119,120</sup> Preliminary near-edge X-ray absorption fine structure measurements suggest that the C–O bond is tilted by  $25 \pm 15^\circ$  with respect to the surface normal, at saturation coverage, although the large uncertainty associated with this determination effectively limits the conclusions that can be drawn.<sup>23</sup> However, these data clearly raise some interesting questions regarding the role of adsorbate structure on reactivity. For example, if only large changes in C–O–Mo bond angle have a significant effect on the reactivity, one might anticipate that the structure of methoxide adsorbed on Mo(100) would be radically different, given that the C–O bond is retained during reaction on this surface. Alternatively, the precise details of the adsorption site may be the dictating factor—clearly considerable mechanistic insight could be gained by companion structural studies of these, and many other, analogous systems.

Secondly, we find that there is no apparent correlation between the relative reactivity of methoxide on various transition metal surfaces and the observed fundamental C–O stretching frequency, *even when the effect of intermolecular coupling is removed*. As discussed earlier, the intermolecular coupling must be normalized for each system, in order that a meaningful comparison can be made. Consequently, data obtained for the same coverage of methoxide on each surface is used, with dipole–dipole removed. In this way, we obtain C–O stretching fundamental frequencies of 980, 1020, and  $<980 \text{ cm}^{-1}$  for 0.1 ML of methoxide adsorbed on Mo(110),<sup>115</sup> Ni(111)<sup>87</sup>, and Cu(100),<sup>121</sup> respectively. Although the facilitation of C–O bond scission on Mo(110) relative to Ni(111) is apparently consistent with the lower frequency on molybdenum, this correlation does not extend to the copper surface, for which decomposition proceeds via partial dehydrogenation to form gaseous formaldehyde, not by C–O bond cleavage as the low-frequency  $\nu(\text{C–O})$  stretching would suggest. In addition, the  $\nu(\text{C–O})$  on Ni(111) is 13  $\text{cm}^{-1}$  lower in frequency than the value in gaseous methanol, previously taken as indicative of a weaker C–O bond, in direct contrast to the reduced anharmonicity observed by overtone

spectroscopy.<sup>122</sup> Clearly, the fundamental frequency alone does not reliably predict the bond strength in these systems. The specific reason for this difference from the known behavior of gas-phase species is not clear, but is most likely due to changes in the *shape* of the intramolecular potential around the equilibrium position that modify the force constant ( $= (d^2 V / dE^2)_0$ ) of a given mode upon adsorption, without affecting the functional form higher in the adsorption well.

## VI. Summary

In this article, we have illustrated how surface vibrational spectroscopy *coupled with* systematic chemical investigations is a powerful combination for the investigation of complex surface reactions. Specifically, recent improvements in the theoretical treatments and technological aspects of vibrational spectroscopy on surfaces has led to significant advances in our ability to understand surface reactions. While only a few cases were used to illustrate the methodology for attacking complex chemical phenomena on metal surfaces, the techniques outlined can be generally applied to the investigation of different classes of reactions on *all* surfaces. As a result of these advances, we may now be entering an era of surface science where more emphasis can be given to understanding a wide array of chemical phenomena.

The next important step in advancing our understanding of complex chemical phenomena will necessarily involve combined theoretical and experimental studies. Theoretical treatments of adsorbate-substrate electronic structure, combined with a normal-mode analysis, will provide a basis for understanding bonding and reactivity on surfaces. Companion studies using vibrational spectroscopy and other structural probes such as photoelectron diffraction, in conjunction with temperature-programmed reaction to measure reactivity, will in turn provide important means of testing the validity of these theoretical analyses.

## VII. Acknowledgments

The authors would like to sincerely thank Yves Chabal for a critical reading of parts of this manuscript and Dr. Cornelis (Kees) Bol, J. P. Frankowski, and Shira Fischer for assistance with figure preparation, and Janis Nader for her assistance with the preparation of this manuscript. In addition, Dr. Cornelis (Kees) Bol and Professor Per Uvdal are acknowledged for their invaluable contributions to the work reviewed herein. We also gratefully acknowledge support of the work reviewed here by the Office of Naval Research (Grant No. N00014-92-J-1841) and The National Science Foundation (CHE-90-06024 and CHE-94-21615).

## VIII. References and Notes

- (1) Bol, C. W. J.; Friend, C. M. *J. Am. Chem. Soc.* **1995**, *117*, 8053–8054.
- (2) Xu, X.; Friend, C. M. *Surf. Sci.* **1992**, *260*, 14–22.
- (3) Brainard, R. L.; Madix, R. J. *Surf. Sci.* **1989**, *214*, 396–406.
- (4) Bowker, M.; Madix, R. J. *Surf. Sci.* **1980**, *95*, 190–206.
- (5) Wachs, I. E.; Madix, R. J. *J. Catal.* **1978**, *53*, 208–227.
- (6) Wachs, I. E.; Madix, R. J. *Surf. Sci.* **1978**, *76*, 531–558.
- (7) Outka, D. A.; Madix, R. J. *J. Am. Chem. Soc.* **1987**, *109*, 1708–1714.
- (8) Sexton, B. A. *Surf. Sci.* **1981**, *102*, 271–281.
- (9) Papapolymerou, G. A.; Schmidt, L. D. *Langmuir* **1987**, *3*, 1098–1102.
- (10) Akhter, S.; White, J. M. *Surf. Sci.* **1986**, *167*, 101–126.
- (11) Attard, G. A.; Chibane, K.; Ebert, H. D.; Parsons, R. *Surf. Sci.* **1989**, *224*, 311–326.
- (12) Ehlers, D. H.; Spitzer, A.; Lueth, H. *Surf. Sci.* **1985**, *160*, 57–69.
- (13) Davis, J. L.; Barteau, M. A. *Surf. Sci.* **1987**, *187*, 387–406.
- (14) Davis, J. L.; Barteau, M. A. *Surf. Sci.* **1988**, *197*, 123–152.
- (15) Davis, J. L.; Barteau, M. A. *Surf. Sci.* **1990**, *235*, 235–248.
- (16) Brown, N. F.; Barteau, M. A. *Langmuir* **1992**, *8*, 862–869.
- (17) Houtman, C. J.; Barteau, M. A. *J. Catal.* **1991**, *130*, 528–546.
- (18) Houtman, C.; Barteau, M. A. *Langmuir* **1990**, *6*, 1558–1566.
- (19) Solymosi, F.; Tarnoczi, T. I.; Berko, A. *J. Phys. Chem.* **1984**, *88*, 6170–6174.
- (20) Xu, X.; Friend, C. M. *Langmuir* **1992**, *8*, 1103–1110.
- (21) Hrbek, J.; dePaola, R. A.; Hoffmann, F. M. *J. Chem. Phys.* **1984**, *81*, 2818–2826.
- (22) dePaola, R. A.; Hrbek, J.; Hoffmann, F. M. *Surf. Sci.* **1986**, *169*, L348–L354.
- (23) Weldon, M. K.; Uvdal, P.; Friend, C. M.; Serafin, J. G. *J. Chem. Phys.* **1995**, *103*, 5075.
- (24) Serafin, J. G.; Friend, C. M. *Surf. Sci.* **1989**, *209*, L163–L175.
- (25) Wiegand, B. C.; Uvdal, P. E.; Serafin, J. G.; Friend, C. M. *J. Am. Chem. Soc.* **1991**, *113* (17), 6686–6687.
- (26) Wiegand, B. C.; Uvdal, P.; Serafin, J. G.; Friend, C. M. *J. Phys. Chem.* **1992**, *96*, 5063–5069.
- (27) Uvdal, P.; Wiegand, B. C.; Serafin, J. G.; Friend, C. M. *J. Chem. Phys.* **1992**, *97* (11), 8727–8735.
- (28) McBreen, P. H.; Erley, W.; Ibach, H. *Surf. Sci.* **1983**, *133*, L469–L474.
- (29) Lu, J.-P.; Albert, M. R.; Bernasek, S. L. *Catal. Lett.* **1990**, *6*, 245.
- (30) Lu, J.-P.; Albert, M. R.; Bernasek, S. L.; Dwyer, D. S. *Surf. Sci.* **1989**, *218*, 1–18.
- (31) Albert, M. R.; Lu, J.-P.; Bernasek, S. L.; Dwyer, D. J. *Surf. Sci.* **1989**, *221*, 197–213.
- (32) Wang, J.; Masel, R. I. *J. Catal.* **1990**, *126*, 519–531.
- (33) Miles, S. L.; Bernasek, S. L.; Gland, J. L. *J. Phys. Chem.* **1983**, *87*, 1626–1630.
- (34) Hofmann, Ph.; Schindler, K. M.; Bao, S.; Fritzsche, V.; Ricken, D. E.; Bradshaw, A. M.; Woodruff, D. P. *Surf. Sci.* **1994**, *304*, 74.
- (35) Lindner, T.; Somers, J.; Bradshaw, A. M.; Kilcoyne, A. L. D.; Woodruff, D. P. *Surf. Sci.* **1988**, *203*, 333–352.
- (36) Woodruff, D. P.; Kilcoyne, A. L. D.; McConville, C. F.; Lindner, T.; Somers, J.; Surman, M.; Bradshaw, A. M. *Vacuum* **1988**, *38*, 305–307.
- (37) Ibach, H.; Mills, D. L. *Electron Energy Loss Spectroscopy and Surface Vibrations*; Academic Press: New York, NY, 1982.
- (38) *Vibrational Spectroscopy of Molecules on Surfaces. Methods of surface characterization*; Yates, J. T., Madey, T. E., Eds.; Plenum Press: New York 1987; Vol 1.
- (39) *Vibrational Spectroscopy of Adsorbates*; Wills, R. F., Vol. Ed.; Springer Series in Chemical Physics 15; Gomer, R., Series Ed.; Springer-Verlag: Berlin, 1980.
- (40) Chabal, Y. J. *Surf. Sci. Rep.* **1988**, *8*, 211–358.
- (41) *Spectroscopy of Surfaces*; Clark, R. J. H., Hester, R. E., Eds.; John Wiley and Sons Ltd.: New York, 1988.
- (42) Champion, J. P.; Robiette, A. G.; Mills, I. M.; Graner, G. *J. Mol. Spectrosc.* **1982**, *96*, 422–441.
- (43) Tong, S. Y.; Li, C. H.; Mills, D. L. *Phys. Rev. Lett.* **1980**, *44*, 407.
- (44) (a) Lee, M. B.; Yang, Q. Y.; Tang, S. L.; Ceyer, S. T. *J. Chem. Phys.* **1986**, *85*, 1693–1694. (b) Yang, Q. Y.; Maynard, K. J.; Johnson, A. D.; Ceyer, S. T. *J. Chem. Phys.* **1995**, *102*, 7734–7749.
- (45) (a) Bent, B. E. *Chem. Rev.* **1996**, *96*, xxxx (this issue). (b) Zaera, F. *Chem. Rev.* **1995**, *95*, 2651–2693. (c) Lin, J.-L.; Bent, B. E. *J. Phys. Chem.* **1993**, *97*, 9713–9718. (d) Lin, J.-L.; Bent, B. E. *J. Am. Chem. Soc.* **1993**, *115*, 2849–2853. (e) Zaera, F. *J. Mol. Catal.* **1994**, *86*, 221–242. (f) Zaera, F.; Tjandra, S. *J. Phys. Chem.* **1994**, *98*, 3044–3049.
- (46) Beckerle, J. D.; Yang, Q. Y.; Johnson, A. D.; Ceyer, S. T. *J. Chem. Phys.* **1987**, *86*, 7236–7237.
- (47) Lee, M. B.; Yang, Q. Y.; Ceyer, S. T. *J. Chem. Phys.* **1987**, *87*, 2724–2741.
- (48) Ceyer, S. T. *Springer Ser. Surf. Sci.* **1990**, *22*, 23–27.
- (49) Beckerle, J. D.; Johnson, A. D.; Ceyer, S. T. *J. Chem. Phys.* **1990**, *93*, 4047–4065.
- (50) Beckerle, J. D.; Johnson, A. D.; Yang, Q. Y.; Ceyer, S. T. *J. Chem. Phys.* **1989**, *91*, 5756–5777.
- (51) Beckerle, J. D.; Johnson, A. D.; Yang, Q. Y.; Ceyer, S. T. *Springer Ser. Surf. Sci.* **1988**, *14*, 109–113.
- (52) Peng, X.; Viswanaathan, R.; Smudde, G. H. J.; Stair, P. C. *Rev. Sci. Instrum.* **1992**, *63*, 3930–3935.
- (53) Smudde, G. H.; Peng, X. D.; Viswanathan, R.; Stair, P. C. *J. Vac. Sci. Technol. A* **1991**, *9* (3), 1885–1889.

- (54) Bol, C. W. J.; Friend, C. M. *Surf. Sci. Lett.* **1995**, *337*, L800–L806.
- (55) Bol, C. W. J.; Friend, C. M. *J. Phys. Chem.* **1995**, *99*, 11930–11936.
- (56) Bol, C. W. J.; Friend, C. M. *J. Am. Chem. Soc.* **1995**, *117* (46), 11572–11579.
- (57) Solymosi, F.; Kovács, I.; Révesz, K. *Surf. Sci.* **1996**, in press.
- (58) Zhou, X.-L.; Liu, Z.-M.; Kiss, J.; Sloan, D. W.; White, J. M. *J. Am. Chem. Soc.* **1995**, *117*, 3565–3592.
- (59) Bugyi, L.; Oszko, A.; Solymosi, F. *J. Catal.* **1996**, in press.
- (60) Friend, C. M.; Xu, X. *Annu. Rev. Phys. Chem.* **1991**, *42*, 251–278.
- (61) The absence of the perturbed  $\nu(\text{C-H})$  mode observed at  $2620\text{ cm}^{-1}$  for methyl on clean Rh(111), when the surface is precovered with oxygen, is consistent with the retardation of the methyl decomposition kinetics in the latter case, since this mode frequency has been shown to be characteristic of “weakened” C–H bonds, as evidenced by the close correlation with the methyl decomposition temperature.<sup>99</sup>
- (62) Lin, J.; Bent, B. E. *Chem. Phys. Lett.* **1992**, *194*, 208.
- (63) Solymosi, F.; Klivenyi, G. *J. Electron Spectrosc. Relat. Phenom.* **1993**, *64/65*, 499–506.
- (64) Bol, C. W. J.; Xu, X.; Friend, C. M. Unpublished results.
- (65) At low oxygen coverages, hydrogenation of the adsorbed alkyl species was also observed due to reaction with surface hydrogen produced (in part) by hydrogen elimination reactions.
- (66) Solymosi et al. assigned a weak peak at  $1050\text{ cm}^{-1}$  to the C–O stretch of adsorbed methoxide in their investigations of methyl iodide on oxygen-covered Pd(100);<sup>57</sup> however, the frequency is not in agreement with earlier investigations of methoxide on the Pd(111)<sup>15</sup> and the spectrum is extremely noisy, suggesting that the peak is not due to methoxide.
- (67) Driessen, M. D.; Grassian, V. H. *J. Phys. Chem.* **1995**, submitted for publication.
- (68) Bol, C. W. J.; Friend, C. M. *Surf. Sci.* **1996**, in press.
- (69) Griller, D.; Kanabus-Kaminska, J. M.; MacColl, A. *J. Mol. Struct.* **1988**, *163*, 125–131.
- (70) Xu, X.; Friend, C. M. *J. Am. Chem. Soc.* **1991**, *113*, 6779–6785.
- (71) Bol, C. W. J.; Friend, C. M. *Surf. Sci. Lett.* **1995**, *322*, L271–L274.
- (72) Bol, C. W. J.; Friend, C. M. *J. Am. Chem. Soc.* **1995**, *117*, 5351–5358.
- (73) The difference in the gas-phase C–X bond strengths of 2-propyl iodide and thiol of  $\sim 16\text{ kcal/mol}$  agrees well with the  $\sim 12\text{ kcal/mol}$  difference in activation energies for reaction of the two molecules on Rh(111)-p(2 $\times$ 1)-O, estimated by a leading-edge analysis of the respective temperature programmed reaction traces, lending additional credibility to the proposed radical mechanism.
- (74) Solymosi, F.; Klivenyi, G. *J. Phys. Chem.* **1995**, *99*, 8950–8953.
- (75) Klivényi, G.; Solymosi, F. *Surf. Sci.* **1995**, *342*, 168.
- (76) Although higher resolution is possible for atoms or diatomics bound to metal surfaces, larger molecules condense on the electron optics and degrade the spectrometer resolution.
- (77) Sexton, B. A. *Surf. Sci.* **1979**, *88*, 299–318.
- (78) Demuth, J. E.; Ibach, H. *Chem. Phys. Lett.* **1979**, *60*, 395–399.
- (79) Witko, M.; Hermann, K.; Ricken, D.; Stenzel, W.; Conrad, H.; Bradshaw, A. M. *Chem. Phys.* **1993**, *177*, 363–371.
- (80) Bhattacharya, A. K.; Chesters, M. A.; Pemble, M. E.; Sheppard, N. *Surf. Sci.* **1988**, *206*, L845–L850.
- (81) Sexton, B. A.; Hughes, A. E.; Avery, N. R. *Surf. Sci.* **1985**, *155*, 366–386.
- (82) Dai, Q.; Gellman, A. J. *J. Phys. Chem.* **1993**, *97*, 10783–10789.
- (83) Dai, Q.; Gellman, A. J. *Surf. Sci.* **1991**, *257*, 103.
- (84) Ryberg, R. *Phys. Rev. B* **1985**, *31*, 2545–2547.
- (85) Stohr, J.; Gland, J. L.; Eberhardt, W.; Outka, D.; Madix, R. J.; Sette, F.; Koestner, R. J.; Doebler, U. *Phys. Rev. Lett.* **1983**, *51*, 2414.
- (86) Chesters, M. A.; McCash, E. M. *Spectrochimica Acta* **1987**, *43A* (12), 1625–1630.
- (87) Zenobi, R.; Xu, J.; Yates, J. T.; Persson, B. N. J.; Volokitin, A. I. *Chem. Phys. Lett.* **1993**, *208*, 414.
- (88) Dastoor, H. E.; Gardner, P.; King, D. A. *Chem. Phys. Lett.* **1993**, *209*, 493–498.
- (89) Schaff, O.; Hess, G.; Fritzsche, V.; Fernandez, V.; Schindler, K.-M.; Theobald, A.; Hoffmann, Ph.; Bradshaw, A. M.; Davis, R.; Woodruff, D. P. *Surf. Sci.* **1995**, *331–3*, 201.
- (90) McKean, D. C. *J. Chem. Soc., Chem. Commun.* **1971**, 1373–1375.
- (91) McKean, D. C. *Spectrochimica Acta* **1973**, *29A*, 1559–1574.
- (92) McKean, D. C.; Duncan, J. L.; Batt, L. *Spectrochimica Acta* **1973**, *29A*, 1037–1049.
- (93) Duncan, J. L.; McKean, D. C.; Speirs, G. K. *Mol. Phys.* **1972**, *24* (3), 553–565.
- (94) Uvdal, P.; Weldon, M. K.; Friend, C. M. *Phys. Rev. B* **1994**, *50*, 12258–12261.
- (95) Weldon, M. K.; Friend, C. M. Proceedings of the 55th Annual Conference on Physical Electronics, Flagstaff, AZ, June 1995.
- (96) The  $C_{3v}$  symmetry refers to the adsorbate. Our experimental observations indicate that the methyl stretch and deformation modes are not sensitive to the symmetry of the surface.
- (97) Sim, W. S.; Gardner, P.; King, D. A. *J. Phys. Chem.* **1995**, *99*, 16002.
- (98) In the study of methoxide on Ag(111),<sup>97</sup> a downshift in the frequency of  $\nu_s(\text{CD}_3)$  of  $27\text{ cm}^{-1}$  was observed on going from physisorbed  $\text{CD}_3\text{OD}$  to chemisorbed  $\text{CD}_3\text{O}^-$ . If a similar shift is applied to the  $\nu_a(\text{CD}_3)$  of  $\text{CD}_3\text{OD}$ , the analogous adsorbate mode would be observed at  $2182\text{ cm}^{-1}$ , in excellent agreement with the observation of an absorbance at  $2185\text{ cm}^{-1}$ , although the authors attribute this feature to  $2\delta(\text{CD}_3)$ . A similar analysis of the data presented for  $\text{CH}_3\text{OH}$  also results in some uncertainty in the reported assignments.
- (99) Weldon, M. K.; Friend, C. M. Manuscript in preparation. Weldon, M. K. Surface Spectroscopy and Chemistry of Intermediates in Catalysis and Diamond Growth on Mo(110). Ph.D. Thesis, Harvard University, Cambridge, MA, 1995.
- (100) This is based on the observation of only a single symmetric C–O stretching mode for all coverages studied, even for the highest resolution ( $1\text{ cm}^{-1}$ ) spectra recorded.
- (101) Persson, B. N. J.; Ryberg, R. *Chem. Phys. Lett.* **1990**, *174*, 443.
- (102) Persson, B. N. J.; Ryberg, R. *Phys. Rev. B: Condens. Matter* **1981**, *24*, 6954–6970.
- (103) Herzberg, G. *Molecular Spectra and Molecular Structure*; Van Nostrand: New York, 1945.
- (104) Richter, L. J.; Germer, T. A.; Sethna, J. P.; Ho, W. *Phys. Rev. B* **1988**, *38*, 10403.
- (105) Guyot-Sionnest, P. *Phys. Rev. Lett.* **1991**, *67*, 2323.
- (106) Andersson, S.; Davenport, J. W. *Solid State Commun.* **1978**, *28*, 677.
- (107) Demuth, J. E.; Schmeisser, D.; Avouris, Ph. *Phys. Rev. Lett.* **1981**, *47*, 1166.
- (108) Lehwald, S.; Ibach, H.; Steininger, H. *Surf. Sci.* **1982**, *117*, 342–351.
- (109) Schmeisser, D.; Demuth, J. E.; Avouris, Ph. *Phys. Rev. B* **1982**, *26*, 4857.
- (110) Steininger, H.; Lehwald, S.; Ibach, H. *Surf. Sci.* **1982**, *123*, 1–17.
- (111) Hoffmann, F. M.; de Paola, R. A. *Phys. Rev. Lett.* **1984**, *52* (19), 1697–1700.
- (112) de Paola, R. A.; Hoffmann, F. M. *Phys. Rev. B* **1984**, *30* (2), 1122–1124.
- (113) Jacobi, K.; Bertolo, M. *Phys. Rev. B* **1990**, *42*, 3733.
- (114) Vattuone, L.; Rocca, M.; Valbusa, U. *Surf. Sci.* **1994**, *314*, L904–L908.
- (115) Uvdal, P.; Weldon, M. K.; Friend, C. M. *Phys. Rev. B* **1996**, *53* (8), 5007–5010.
- (116) Andersson, S.; Persson, B. N. J. *Phys. Rev. Lett.* **1980**, *45*, 1421–1424.
- (117) This is only strictly true if the surface Brillouin zone possesses inversion symmetry.
- (118) Serrallach, A.; Meyer, R.; Gunthard, H. H. *J. Mol. Spectrosc.* **1974**, *52*, 94–129.
- (119) Uvdal, P.; MacKerell, A. D., Jr.; Wiegand, B. C.; Friend, C. M. *Phys. Rev. B* **1995**, *51*, 7844–7848.
- (120) Uvdal, P.; MacKerell, A. D., Jr.; Wiegand, B. C. *J. Electron Spectrosc. Relat. Phenom.* **1993**, *64/65*, 193–199.
- (121) Ryberg, R. *J. Chem. Phys.* **1985**, *82*, 567–573.
- (122) This discrepancy is not due to mechanical renormalization effects, which result from the additional mass associated with the extended surface, since that would give rise to an increase in the observed frequency.

